



VICTORIA UNIVERSITY
MELBOURNE AUSTRALIA

Ensemble neural network approach detecting pain intensity from facial expressions

This is the Accepted version of the following publication

Bargshady, Ghazal, Zhou, X, Deo, Ravinesh C, Soar, Jeffrey, Whittaker, Frank and Wang, Hua (2020) Ensemble neural network approach detecting pain intensity from facial expressions. *Artificial Intelligence in Medicine*, 109. ISSN 0933-3657

The publisher's official version can be found at
<https://www.sciencedirect.com/science/article/pii/S0933365720312197?via%3Dihub>
Note that access to this version may require subscription.

Downloaded from VU Research Repository <https://vuir.vu.edu.au/42258/>

Manuscript Details

| | |
|--------------------------|---|
| Manuscript number | AIIM_2020_86_R3 |
| Title | Ensemble neural network approach detecting pain intensity from facial expressions |
| Article type | Research Paper |

Abstract

This paper reports on research to design an ensemble deep learning framework that integrates fine-tuned, three-stream hybrid deep neural network (i.e., Ensemble Deep Learning Model, EDLM), employing Convolutional Neural Network (CNN) to extract facial image features, detect and accurately classify the pain. To develop the approach, the VGGFace is fine-tuned and integrated with Principal Component Analysis and employed to extract features in images from the Multimodal Intensity Pain database at the early phase of the model fusion. Subsequently, a late fusion, three layers hybrid CNN and recurrent neural network algorithm is developed with their outputs merged to produce image-classified features to classify pain levels. The EDLM model is then benchmarked by means of a single-stream deep learning model including several competing models based on deep learning methods. The results obtained indicate that the proposed framework is able to outperform the competing methods, applied in a multi-level pain detection database to produce a feature classification accuracy that exceeds 89%, with a receiver operating characteristic of 93%. To evaluate the generalization of the proposed EDLM model, the UNBC-McMaster Shoulder Pain dataset is used as a test dataset for all of the modelling experiments, which reveals the efficacy of the proposed method for pain classification from facial images. The study concludes that the proposed EDLM model can accurately classify pain and generate multi-class pain levels for potential applications in the medical informatics area, and should therefore, be explored further in expert systems for detecting and classifying the pain intensity of patients, and automatically evaluating the patients' pain level accurately.

| | |
|---|--|
| Keywords | ensemble neural network; pain detection; facial expression; deep learning |
| Manuscript region of origin | Asia Pacific |
| Corresponding Author | Ghazal Bargshady |
| Corresponding Author's Institution | University of Southern Queensland (USQ) |
| Order of Authors | Ghazal Bargshady, Xujuan Zhou, Ravinesh Deo, Jeffrey Soar, Frank Whittaker, Hua Wang |

Submission Files Included in this PDF

File Name [File Type]

Title Page.docx [Cover Letter]
response letter - R2.docx [Response to Reviewers]
Highlightes.docx [Highlights]
revised-manuscript - R2.docx [Manuscript File]
Figures - R2.docx [Figure]
Tables - R2.docx [Table]
declaration-of-competing-interests.docx [Conflict of Interest]

To view all the submission files, including those not included in the PDF, click on the manuscript title on your EVISE Homepage, then click 'Download zip file'.

Research Data Related to this Submission

There are no linked research data sets for this submission. The following reason is given:
The authors do not have permission to share data

An ensemble neural network approach to detect pain intensity from facial expressions

Ghazal Bargshady (ghazal.bargshady@usq.edu.au)^{a*}, **Xujuan Zhou** (xujuan.zhou@usq.edu.au)^a, **Ravinesh C Deo** (ravinesh.deo@usq.edu.au)^b, **Jeffrey Soar** (jeffrey.soar@usq.edu.au)^a, **Frank Whittaker** (Frank.Whittaker@usq.edu.au)^a, **Hua Wang** (Hua.Wang@vu.edu.au)^c

^a School of Management and Enterprise
University of Southern Queensland
Springfield, Qld 4300, Australia

^b School of Sciences
University of Southern Queensland
Springfield, Qld 4300, Australia

^c Victoria University, Melbourne, Australia

*Corresponding author: Ghazal Bargshady, email: ghazal.bargshady@usq.edu.au, phone: (+61)(405)(415-178), address: 37 Sinnathamby Blvd, Springfield Central QLD 4300, University of Southern Queensland (USQ) Springfield campus

AIIM: Editorial Decision on AIIM_2020_86_R2

An ensemble neural network approach to detect pain intensity from facial expressions

To

Professor Carlo Combi

Editor-in-Chief for Artificial Intelligence in Medicine

Re: Revised Manuscript AIIM_2020_86_R2

Dear Prof Combi

The authors would like to express their gratitude to reviewers and the journal editorial board.

The authors also thank you for the opportunity to revise the manuscript.

The authors have carefully considered all the comments. In response, we have revised the paper carefully, ensuring the reviewers' comments are addressed properly. The revisions made to this paper can be tracked in the revised manuscript as they are written in **green** font.

In the revised document, we also provide our response all the reviewers' comments, which is presented in the table below. The left side shows the comments from the reviewers and the right-hand side shows the author responses demonstrating how the necessary revisions were made.

Reviewer_1

| | Reviewer Comment(s) | Author Responses |
|---|---|---|
| 1 | In Fig.6, you have to present the same person for each level. | Done. Figure 6 has been updated as the review mentioned by a same person for each level. Please see line 303. |
| 2 | In Fig. 7, also you have to present the same person for each level. Actually, In Fig. 6 and Fig.7 some images are looks like reused for different level image. | Done. Figure 7 has been updated as the review mentioned by a same person for each level. Please see line 314. |

Reviewer_2

| | Reviewer Comment(s) | Author Responses |
|---|--|---|
| 1 | Line 646: References are re-indexed from 1. | Thanks for picking this issue. References issue has been fixed. |
| 2 | Line 214, 223, 225, 235 should start with lower case character. | Done. Please see the lines 211, 220, 222, 232. |
| 3 | Line 221: what is X []? | Corrected. Please see line 218. |
| 4 | Line 274: should move the table caption to next page | Done. Please see line 271. |
| 5 | Line 280: should be " Experimental configuration and databases"? | Fixed. Please see line 277. |
| 6 | Line 288: should be "The MIntPAIN database"? | Fixed. Please see line 285. |

The authors wish to thank you for multiple rounds of revisions of our paper.

We hope now the paper can be accepted for publication.

Sincerely

Ghazal Bargshady, 20/08/2020

On behalf of all co-authors

Highlights:

- Automated detection of pain from facial expressions is a challenge in medical care.
- A new ensemble deep neural network algorithm designed to improve automatic pain detection.
- The performance of the new proposed ensemble deep learning algorithm for detecting pain in 5 level is high and tested in two different databases.

Ensemble neural network approach detecting pain intensity from facial expressions

Ghazal Bargshady (ghazal.bargshady@usq.edu.au)^{a*}, Xujuan Zhou (xujuan.zhou@usq.edu.au)^a, Ravinesh C Deo (ravinesh.deo@usq.edu.au)^b, Jeffrey Soar (jeffrey.soar@usq.edu.au)^a, Frank Whittaker(Frank.Whittaker@usq.edu.au)^a, Hua Wang(Hua.Wang@vu.edu.au)^c

^a School of Management and Enterprise
University of Southern Queensland
Springfield, Qld 4300, Australia

^b School of Sciences
University of Southern Queensland
Springfield, Qld 4300, Australia

^c Victoria University, Melbourne, Australia

*Corresponding author: Ghazal Bargshady, email: ghazal.bargshady@usq.edu.au, phone: (+61)(405)(415-178), address: 37 Sinnathamby Blvd, Springfield Central QLD 4300, University of Southern Queensland (USQ) Springfield campus

Abstract

This paper reports on research to design an ensemble deep learning framework that integrates fine-tuned, three-stream hybrid deep neural network (*i.e.*, Ensemble Deep Learning Model, EDLM), employing Convolutional Neural Network (CNN) to extract facial image features, detect and accurately classify the pain. To develop the approach, the VGGFace is fine-tuned and integrated with Principal Component Analysis and employed to extract features in images from the Multimodal Intensity Pain database at the early phase of the model fusion. Subsequently, a late fusion, three layers hybrid CNN and recurrent neural network algorithm is developed with their outputs merged to produce image-classified features to classify pain levels. The EDLM model is then benchmarked by means of a single-stream deep learning model including several competing models based on deep learning methods. The results obtained indicate that the proposed framework is able to outperform the competing methods, applied in a multi-level pain detection database to produce a feature classification accuracy that exceeds 89%, with a receiver operating characteristic of 93%. To evaluate the generalization of the proposed EDLM model, the UNBC-McMaster Shoulder Pain dataset is used as a test dataset for all of the modelling experiments, which reveals the efficacy of the proposed method for pain classification from facial images. The study concludes that the proposed EDLM model can accurately classify pain and generate multi-class pain levels for potential applications in the medical informatics area, and should therefore, be explored further in expert systems for detecting and classifying the pain intensity of patients, and automatically evaluating the patients' pain level accurately.

Keywords: ensemble neural network, pain detection, facial expression, deep learning

1. Introduction

Pain is a significant indicator of human discomfort and an indicator of the need for medical diagnosis of a possible disease and its related treatments in patients. It is usually measured by clinicians, albeit, employing largely a manual approach such as using a self-reported pain detection system. Various pain measurement scales have been designed to describe a patient’s self-report of pain intensity, including but not limited to the Visual Analogue Scale (VAS)¹, Verbal Rating Scale (VRS), Faces Pain Scale-Revised (FPSR), and the Numerical Rating Scale (NRS) [1]. However, self-reported pain level assessment may not always be the appropriate method for different disease contexts and patients’ scenarios [1, 2]. Moreover, in doing so, this task may require greater intellectual and dialectal abilities that makes the self-reporting impractical for populations such infants and elderly patients lacking effective communication skills [3, 4]. An automated decision support system for pain assessment that utilises facial image processing can provide an effective alternative medium to the self-reporting method to more accurately evaluate the severity of pain. Two examples of such systems include the Facial Action Coding System (FACS) [5] and the Prkachin and Solomon Pain Intensity (PSPI) scale [6]. However, automatically assessing the pain level from facial images or video recordings can be a challenging task because of the presence of several external and complicating factors (*e.g.*, phenomenon of human smiles in spite of pain and the gender related pain tolerating abilities [7]). **This means that we are likely to face a major challenge in terms of accurate facial expression recognition and interpretation due to the relatively large visual features with considerable variation caused by person-to-person characteristics, their expressions and the variations in face appearance caused by many extrinsic conditions such as illumination and the point of view [8]. Another key challenge in facial expression recognition arises from the need to develop effective representation that balance the complex distribution of intra- and inter- class variations [9]. Effective methods that demarcate true facial features associated with a pain level and the causal factor (*i.e.* medical condition) are highly warranted to support rapidly evolving medical informatics capabilities.**

List of acronyms

AAM (Active Appearance Models)
ARC (Australian Research Council)
ASM (Active Shape Model)
AUC (Area under Curve)
BiLSTM (Bidirectional Long Short Memory)
CNN (Convolutional Neural Network)
D (Depth)
EDLM (Ensemble Deep Learning Model)
FACS (Facial Action Coding Systems)
FN (False Negative)
FP (False Positive)
FPR (False Positive Rate)
FPSR (Faces Pain Scale-Revised)
LBP (Local Binary Pattern)
LSTM (Long Short-Term Memory)

MAE (Mean Absolute Error)
MIntPAIN (Multimodal Intensity Pain)
MSE (Mean Squared Error)
NRS (Numerical Rating Scale)
PCA (Principal Components Analysis)
RNN (Recurrent Neural Network)
PSPI (Prkachin and Solomon Pain Intensity)
ROC (Receiver Operating Characteristics)
SVM (Support Vector Machine)
TN (True Negative)
TP (True Positive)
TPR (True Positive Rate)
T (Thermal)
VRS (Verbal Rating Scale)
VAS (Visual Analogue Scale)

26 Artificial intelligence (AI) algorithms in an automatic pain detection system that analyse concealed
27 features using indicators of pain (*e.g.*, a face image) can potentially provide medical practitioners a
28 more intelligent approach to investigate the actual pain level prior to treating the relevant disease.
29 Recently, deep learning methods employing multiple hidden layer neuronal systems for feature
30 extraction have gained importance as a mainstream automated technique for this purpose, with its
31 increasing capacities to perform complex and highly nonlinear predictive modelling tasks (*e.g.*,
32 classification and feature extraction) from relatively complex datasets such as human face images that
33 indicate a medical condition. Many deep learning techniques, including convolutional neural networks
34 (CNN) [10], and recurrent neural networks (RNN) [11], have thus been explored for facial expression
35 analysis and pain detection.

36 In spite of many AI methods tested for feature extraction, the ensemble-based approaches where two or
37 more algorithms are integrated to capture the merits of each for improved accuracy is being widely
38 developed for multi-purpose classification tasks [12, 13]. The popularity of ensemble-based methods is
39 perhaps attributable to their relatively superior performance in comparison to the other single deep
40 learning algorithms. The study of [14] provided three important reasons to adopt this method, including
41 their statistical, computational, and representational efficacy compared to single algorithm learning
42 models. Indeed, increasing the number of stacked hidden layers and neuronal networks depth can
43 improve the clarity of features learned from the CNNs and, and therefore, improving the performance
44 of deep neural networks in image processing tasks [15]. Therefore, in this research paper we aim to
45 build and test a new ensemble deep learning model to recognise the multi-classification level pain
46 intensity employing the patient's video frame images.

47 [The proposed ensemble model consists of two steps including feature extraction as early fusion and](#)
48 [classification as late fusion.](#) In the early fusion section, a newly developed feature extraction technique
49 has been applied based on the fine-tuned VGGFace algorithm that integrates Principal Component
50 Analysis (PCA) hieratically to extract the features embedded in human face images. Henceforth, in the
51 late fusion section, a three-stream CNN-RNN network has been designed, and finally, the resulting
52 facial image features are merged as the output of the ensemble classification model. The proposed
53 algorithm is tested comprehensively by employing two unique databases. First the Multimodal Intensity
54 Pain (MIntPAIN) database [2, 16] with labelled video sequences in terms of the VAS metric and second,
55 the UNBC-McMaster Shoulder Pain Archive Dataset [17] with labelled video frames in terms of PSPI
56 and FACS metrics are used.

57 More precisely, the novelty of this research is as follows:

- 58 1) A new image classification approach with an early fusion section is constructed for effective
59 feature extraction by adopting the fine-tuning VGG-Face pre-trainer, and its outputs are

60 integrated with PCA to extract the features more effectively and efficiency by reducing the
61 dimensionality of image dataset.

62 2) A new image classification approach that includes a three-stream ensemble CNN-RNN
63 classifier system, where the outputs are merged by means of the late fusion section to finally
64 classify the pain level in five distinct levels, resulting from the extracted features from human
65 facial images.

66 3) The overall framework denoted as Ensemble Deep Learning Model (EDLM) model is trained
67 and tested utilising two popular face databases represented with various pain features and the
68 obtained results are used to benchmark EDLM against state-of-the-art techniques as the
69 baseline model.

70 The rest of the paper is organized as follows: In Section 2, the existing methods and related works are
71 described. In Section 3, an overview of the proposed EDLM model is introduced. Next, the experiments
72 and databases are presented in Section 4 while the results and discussions are provided in Section 5,
73 with conclusions and future works outlined in Section 6.

74 **2. Related works**

75 In the following, the related studies in pain detection from facial expressions, including a general
76 overview of deep learning techniques, existing research and ensemble neural networks are described.

77 **2.1 Deep learning used in facial expressions**

78 CNNs have been used to image classification and applied to identify face and objects effectively [18,
79 19]. CNNs and their pre-trained algorithms obtained notable results especially in image classification
80 and feature extraction [20]. In addition, recently CNNs models have achieved higher performances on
81 the ImageNet dataset such as AlexNet [10], GoogLeNet [21]. Features extracted from pre-trained CNNs
82 used in computer vision tasks such as emotion recognition and object detection and the achieve results
83 indicated better performance in comparison with handcrafted features.

84 Even though deep learning methods are powerful tools for tasks estimation, however; they are not
85 suitable for analysing sequential data such as speech or video data. Therefore, RNN was designed to
86 represent features in capturing information from all the earlier time steps and to renew its representation
87 through upcoming information [22]. Long short-term memory (LSTM) deep learning is based on RNN
88 architecture and unlike feedforward neural networks it has feedback connection. Standard RNNs can
89 learn based on long-term dependencies like LSTM but training them is difficult since the gradients tend
90 to vanish or explode. LSTM has a cell state under control by three gates as: forget, input, and output
91 gates. The Forget gate keeps relevant information from prior steps. The input gate adds relevant
92 information from the current step. The output gate determines the next hidden state status [23, 24]. Fig.
93 1 shows the architecture of an LSTM cell, in which the cell state part is calculated by:

94
$$i_t = \sigma(W_{xi}x_t + W_{hi}h_{t-1} + W_{ci}c_{t-1} + b_i) \quad (1)$$

95 The output of the forget gate is calculated as:

96
$$f_t = \sigma(W_{xf}x_t + W_{hf}h_{t-1} + W_{cf}c_{t-1} + b_f) \quad (2)$$

97 The cell state for the current time-step is calculated as following:

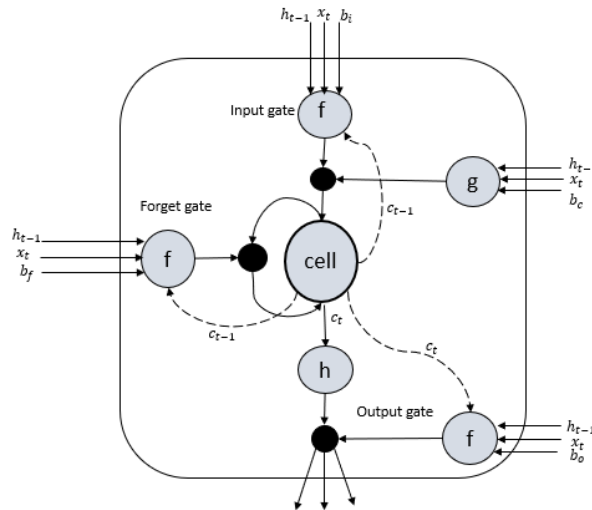
98
$$c_t = f_t c_{t-1} + i_t \tanh(W_{xc}x_t + w_{hc}h_{t-1} + b_c) \quad (3)$$

99 Once the forget and input gates have controlled the amount of information in the earlier cell state c_{t-1}
 100 and the new cell state c_t should be let through.

101 The state can expect the output of the cell as following:

102
$$o_t = \sigma(W_{xo}x_t + W_{ho}h_{t-1} + W_o c_t + b_o) \quad (4)$$

103
$$h_t = o_t \tanh(c_t) \quad (5)$$



104

105 **Fig. 1.** The architecture of an LSTM unit [23, 24]
 106 Inputs: x_t : Input vector, c_{t-1} : memory from previous block, h_{t-1} : output of previous block, b : Bias
 107 Outputs: h_t : the output of current block, c_t : memory from the current block

108 Access to both past (left) and future frames is essential for sequences labelling tasks. However, the
 109 LSTM's hidden state h_t takes information only from the past frame, without having information from
 110 the future frame. Bidirectional LSTM (BiLSTM) [25] as an elegant solution presents each sequence
 111 forwards and backwards as two separate hidden states to capture past and future information,
 112 respectively.

113 **2.2 Existing automate pain detection models from facial expressions**

114 Various deep learning (*i.e.*, multiple hidden layer) and non-deep learning (*i.e.*, single hidden layer)
 115 approaches have been proposed to detect pain from facial expressions, with significant progress made

116 in this research area recently. In terms of classification problems, some traditional non-deep learning
117 algorithms such as Support Vector Machine (SVM) have been used for the classification of features in
118 facial expressions. In terms of non-deep learning feature extraction techniques, Active Appearance
119 Models (AAM) and Active Shape Model (ASM), Gabor wavelets, Local Binary Pattern (LBP) were
120 applied to extract features for this task. For example, [26, 27] used AAM based features combined with
121 SVM classifiers for pain detection. [28, 29] applied Gabor wavelets as the main components of their
122 filter banks and LBP features with SVMs, respectively.

123 Recently, with major progress in deep learning abilities and increasingly available large training data
124 to work with, deep learning algorithms, which have a good ability to reveal intrinsically concealed
125 patterns in complex datasets (*e.g.*, images), have been applied in feature extraction and classification
126 problems. Deep models such as convolutional networks and deep belief and are recognized to improve
127 feature extracting process [10, 30]. For example, significantly accurate results were achieved in pain
128 detection from facial expression by using a pre-trained CNN for features extraction in the UNBC-
129 McMaster Shoulder Pain Archive database [17]. Furthermore, [22] proposed a real-time regression
130 framework based on the RNN to estimate pain levels from facial expressions by extracting features
131 from pre-trained CNN and combining them with RNN as a new model. Using the same technique, [31,
132 32] extracted facial features from pre-trained VGGFaces, and then integrated them into a LSTM to
133 utilize the temporal relationships between video frames. In a new and different painful facial expression
134 database MIntPAIN [2, 16], a pre-trained CNN (VGGFace) and LSTM were applied in a fusion
135 algorithm for spatial-temporal analysis considering Depth (D), and Thermal (T) accompanied by
136 chromatic (RGB) video data to detect pain in five classes. In [33], a three stream network with three
137 different feature extraction techniques including the appearance Histogram of Oriented Gradients
138 (HOG), CNN, and the shape features using handcrafted algorithms and the Relevance Vector Machines
139 (RVM) used to estimate the pain. In [34], proposed an automated pain detection system including two
140 machine learning systems: an Automated Facial Expression Recognition (AFER) system that computes
141 the frame-level confidence scores for single AUs and a Multiple Instant Learning (MIL) system that
142 performs the sequence-level pain prediction based on contributions from a pain-relevant set of AU
143 combinations. More details about the automatic pain recognition approaches are explained in a survey
144 paper published recently [35].

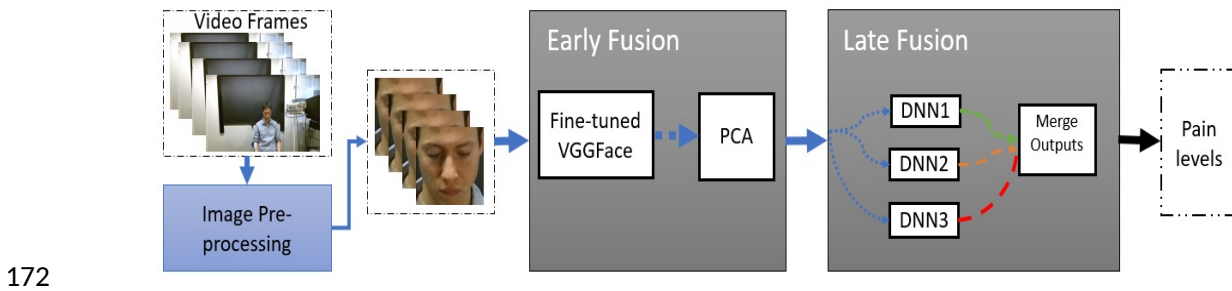
145 **2.3 Ensemble neural networks**

146 An ensemble model, following notion of ‘*The Wisdom of Crowds*’, can be described as a composition
147 of multiple weak learners to form one single learner with expected higher predictive performance. The
148 weak learner is defined as a learner that performs slightly better than random guessing [36]. Ensembles
149 of learning algorithms have been effectively used in many computer vision problems to improve the
150 classification performance [15, 37]. According to [14] ensemble learning is effective method since: “1)

151 the training phase does not provide enough data to shape a single finest classifier; 2) an ensemble using
 152 separate starting points could better estimated the finest result; 3) an ensemble may expand space for a
 153 better approximation”. Also, ensemble learning algorithms improve the generalization ability. Ding and
 154 Tao (2017), used ensemble CNN for video-based face recognition [38]. Their model outperforms
 155 previous approaches such as Deep Face [18], DeepID2+ [19], and VGG Face [39]. According to [40],
 156 , a neural network ensemble can be designed by altering the initial weights, the network architecture,
 157 and the training set. The combined decision created by the ensemble method is less expected error than
 158 the decision produced by other individual networks [41]. A Horizontal and Vertical Ensemble methods
 159 proposed to enhance the classification performance of deep neural networks. Based on their results both
 160 linear Horizontal Voting and Horizontal Stacked Ensemble methods can strongly enhance the
 161 performance of deep learning classification [42].

162 3. The proposed ensemble deep learning framework

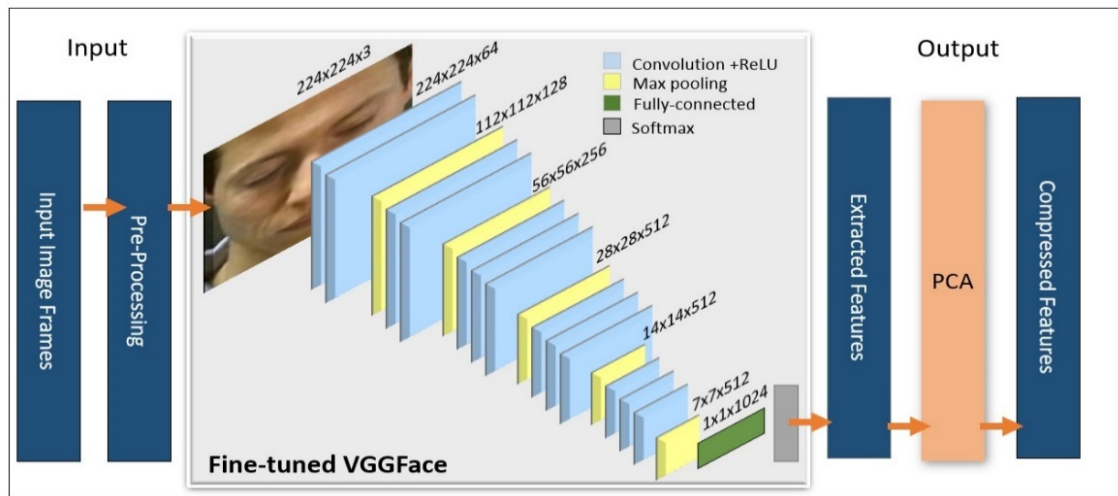
163 The novelty of this study is to propose a new ensemble deep learning model (EDLM) to classify pain
 164 intensity in multi-levels (five classes) from facial expression video frames data. The block diagram of
 165 the proposed system is shown in Fig. 2. The pre-processing and normalization are applied on dataset
 166 before feeding the images into the proposed deep learning model. The EDLM consists of two sections
 167 including the early fusion and late fusion. In the early fusion, a combination of pre-trained CNN and
 168 linear PCA is used to extract and select features. Then, the extracted features are transferred in the late
 169 fusion for classification. An ensemble three stream CNN+RNN hybrid deep learning network is used
 170 in late fusion to classify pain levels in five classes. In the following, the details of the early fusion, late
 171 fusion, and entire EDLM algorithm is explained.



173 **Fig. 2.** Block diagram of the proposed ensemble deep learning model (EDLM) to detect pain in multi-classes
 174 from facial expressions.

175 3.1 Early fusion

176 To design the proposed EDLM model, the first step is to design early fusion feature extraction section.
 177 In addition, the pre-processed data is transferred in the early fusion algorithm to extract features. The
 178 early fusion section contains of the fine-tuned VGGFace pre-trained with Faces [39] which its outputs
 179 combined with PCA (see Fig. 3).



181

182 **Fig. 3.** Early fusion step of the EDLM for feature extraction and selection by integration fine-tuned VGGFace
 183 and PCA

184

185 In the computer vision field, transfer learning is usually expressed using pre-trained models such as a
 186 model trained on a large benchmark dataset to solve a problem. Several of the state-of-the-art techniques
 187 used transfer learning solution to generate results in image classification [10]. The VGGFace has five
 188 convolution blocks and three fully connected layers (fc6, fc7, and fc8). For fine-tuning it, a Dense
 189 connected model at top of the VGGFace model is created and the convolution layers are freeze, then
 190 data normally fed to the network [43]. Convolution neural networks-based methods can derive deep
 191 feature extraction from a set of training images. However, one challenge in this task is that the
 192 dimension of the extracted image features can increase dramatically with the addition of more network
 193 layers [44]. To resolve this problem, after using deep learning to extract image features, the PCA
 194 algorithm is used in this study to achieve dimension reduction. The study adopts PCA, as it is a
 195 dimensionality reduction method that is useful for diverse applications (*e.g.*, image compression, facial
 196 feature extraction, face recognition and finding the patterns from large dimensional images) [45, 46].
 197 This method can also help us choose the best set of data dimensions that will make the model perform
 198 better, and to increase efficiency of the algorithm performance [47]. There is a total of 125280 features,
 199 which have been extracted from the training data set, calculated according to the input shape of the
 200 extracted features. For the training data set, these are denoted as (31320, 4) where the number 34800
 201 refers to the number of training images and so, we are able to obtain a product $31320 \times 4 = 125280$.
 202 In addition, the 4 distinct output features (per image) extracted from the fine-tuned VGG-Face are
 203 transferred into the PCA algorithm with an aim to reduce the dimensionality of the extracted features
 204 and also to increase efficiency of the classification algorithm. It would thus be of interest to be able to
 205 discover “sparse principal components” such as sparse vectors spanning a low-dimensional space. To

206 achieve this, it is necessary to reduce some of the explained variance and the orthogonality of the
207 principal components. The explained variance for each component is calculated by Python software.

208 The dimensionality reduction process is achieved through an orthogonal, linear projection operation.
209 Without loss of generality, the PCA operation can be defined as [48]:

$$210 \quad Y = XC \quad (6)$$

211 with

$$212 \quad Y \in R^{S \times P}$$

213 is the projected data matrix that contains P principal components of X with,

$$214 \quad P \leq N.$$

215 So, the key is to find the projection matrix

$$216 \quad C \in R^{N \times P}$$

217 which is equivalent to find the eigenvectors of the covariance matrix of X , or alternatively solve a singular
218 value decomposition (SVD) problem for X .

$$219 \quad X = U\Sigma V^T \quad (7)$$

220 where

$$221 \quad U \in R^{S \times S}$$

222 and

$$223 \quad V \in R^{N \times N}$$

224 are the orthogonal matrices for the column and row spaces of X , and Σ is a diagonal matrix containing
225 the singular values,

$$226 \quad \lambda_n, \quad \text{for } n = 0, \dots, N-1$$

227 non-increasingly lying along the diagonal. It can be shown that the projection matrix C can be obtained
228 from the first P columns of V with

$$229 \quad V = [v_1, \dots, v_N] \quad (8)$$

230 and

$$231 \quad C = [c_1, \dots, c_P] \quad (9)$$

232 where

$$233 \quad v_n \in R^{N \times 1}$$

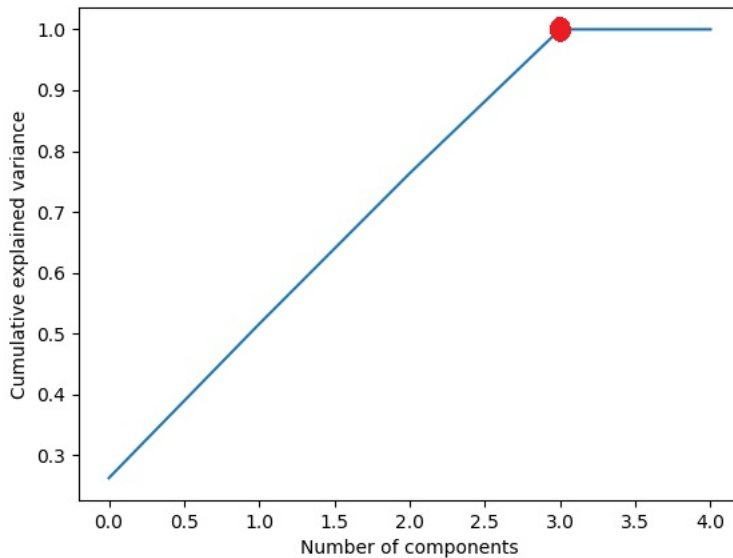
234 is the n^{th} right singular vector of X , and

235
$$c_n = v_n.$$

236 In fact, the singular values contained in Σ are the standard deviations of X along the principal directions
237 in the space spanned by the columns of C . Therefore, λ_n^2 becomes the variance of X projection along the
238 n^{th} principal component direction. It is believed that variance can be explained as a measurement of how
239 much information a component contributes to the data representation. One way to examine this is to look
240 at the cumulative explained variance ratio of the principal components, given as [48]:

241
$$R_{cev} = \frac{\sum_{n=1}^P \lambda_n^2}{\sum_{n=1}^N \lambda_n^2} \quad (10)$$

242 Fig. 4 describes that selecting 3 components can preserve majority of the total variance of the input
243 data. A vital part of using PCA in practice is the ability to estimate how many components are needed
244 to describe the data. This can be determined by looking at the cumulative *explained variance ratio* as a
245 function of the number of components. This graph quantifies how much of the total, 4-dimensional
246 variance is contained within the components. For example, we see that with the first 1 component
247 contain approximately 48% of the variance, while we need around 3 components to describe close to
248 100% of the variance.



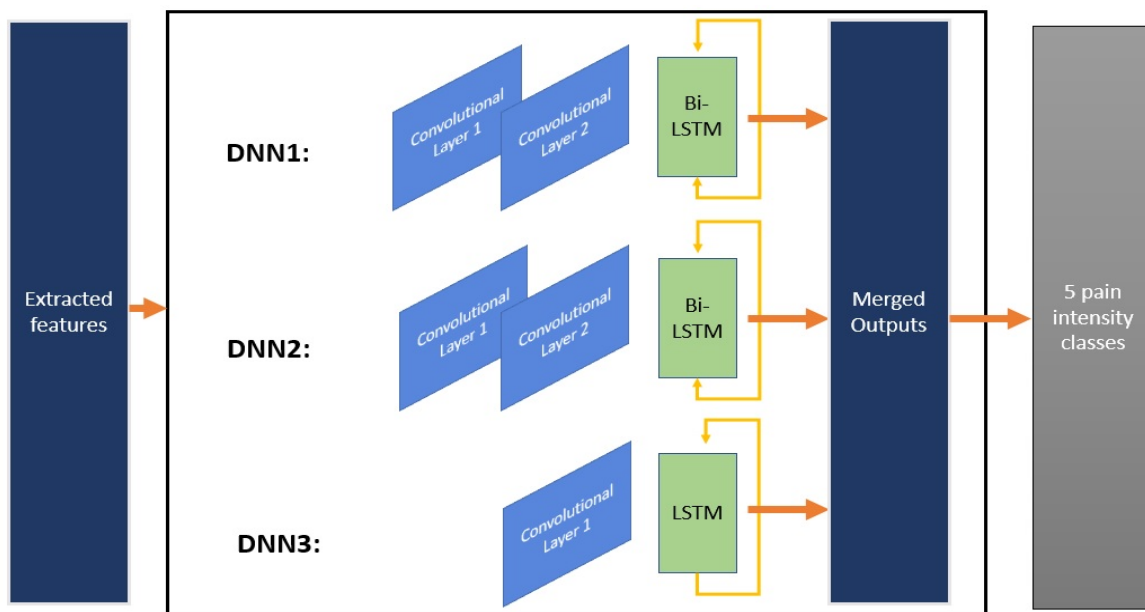
249

250 **Fig. 4.** Number of components to select from extracted features by PCA

251 **3.2 Late fusion section**

252 In the late fusion part of the proposed EDLM used as the classification section, an ensemble deep
 253 learning network is designed in varying initial weights and network architecture. As discussed in the
 254 *Related Works* section, ensemble learning is an effective method and can improve the generalization
 255 ability of classification. Since the data is video and contains video image frames, and RNNs suited for
 256 sequential data we used temporal information to feed into RNNs. The training of RNNs act as back-
 257 propagation algorithm [25].

258 The proposed algorithm was tested in a different version. The experimental results indicated that using
 259 hybrid CNN+RNN in late fusion has more accurate results than networks that only include RNN in late
 260 fusion. Therefore, three independent and hybrid CNN+RNN deep learning methods are designed and
 261 their outputs are merged. The merged output used to classify pain intensity. These three independent
 262 and hybrid deep learning networks are DNN1, DNN2, and DNN3 which are developed using different
 263 parameter, weight, and architecture. The configurations of these networks are described in Table 1. As
 264 can be seen from Table 1, DNN1 and DNN2 contain two CNNs with Conv2D architecture which their
 265 output shift in stack way to a BiLSTM. However, DNN1 and DNN2 are different in weighting. For
 266 DNN3, a different architecture of CNN+RNN is used. In addition, a CNN with Conv1D is selected and
 267 its output is transferred into a LSTM. Fig. 5 illustrates the late fusion architecture of the proposed EDLM
 268 model.



269

270

Fig. 5. Late fusion step of the EDLM based on ensemble deep neural network.

Table 1. Properties of DNN1, DNN2, and DNN3 proposed in the late fusion stage.

| DNN | Convolution layer 1 | Convolution layer 2 | RNN |
|------|---|--|---|
| DNN1 | type = conv2d, filter number = 256, activation = ReLU, input shape = (1,5) | type = conv2d filter number = 256, activation = ReLU, input shape = (1,5) | type = BiLSTM, filter number = 256, dense = 4096, drop out = 0.5, activation = ReLU |
| DNN2 | type = conv2d, filter number = 128, activation = ReLU, input shape = (1,5) | type = conv2d filter number = 128, activation = ReLU, input shape = (1,5) | type = BiLSTM, filter number = 32, dense = 4096, drop out = 0.5, activation = ReLU |
| DNN3 | type = conv1d, filter number = 256, activation = ReLU, input shape = (1,5) | None | type = BiLSTM, filter number = 128, dense = 4096, drop out = 0.5, activation = ReLU |

272 3.3 The EDLM algorithm design

273 The details of the proposed EDLM method are summarized in Algorithm 1. During experimentation
 274 optimization for the early fusion feature extraction section, the model ran by 50 epoch and 48 batches.
 275 However, in the late fusion, the model performed by 5 epoch and 48 batches. To estimate the skill of
 276 the algorithm, the cross-validation method involved by repeating 10 times.

Algorithm 1: The proposed EDLM algorithm

```

1: Procedure EDLM (input, n, j, batch)
2:   Pre-process (input)
3:   for k ← 0, n do
4:     finetune (VGG-Face)
5:     for epoch ← 0, j do
6:       features ← train (finetune (VGG-Face))
7:     end for
8:     SF ← PCA (features)
9:     GN ← Calculate (GN)
10:    for epoch ← 0, j do
11:      o1 ← DNN1(SF)
12:      o2 ← DNN2(SF)
13:      o3 ← DNN3(SF)

```

```
14:         out ← merge (o1, o2, o3)
15:         out ← GN (48)
16:         train (model (SF, out))
17:     end for
18: end for
19: end procedure
```

277 4. Experimental configuration and databases

278 In this study, the objective algorithm (EDLM) and all the other comparative algorithms are built under
279 an Intel core *i7 @* 3.3 GHz and 16 GB memory computer. *Python software* [49] was used for the model
280 construction and prototyping, since it has freely available libraries suits for deep learning such as *Keras*
281 [50], *TensorFlow* [51], *Scikit-learn* [52], *Matplotlib* [53]. *Keras* allows for easy and fast prototyping
282 and supports both convolutional networks and recurrent networks. *Matplotlib* as a *Python* 2D plotting
283 library is used for plotting and statistical analysis of modelling data. The selected database and
284 evaluation metrics are explained as following.

285 4.1 The MIntPAIN database

286 To establish the robustness of the proposed EDLM model, we used two databases includes the
287 MIntPAIN database [2, 16] and the UNBC-McMaster Shoulder Pain dataset [17]. The MIntPAIN
288 database includes pain video data taken by electrical stimulation in five levels (Level 0 no pain, and to
289 Level 4 is the highest level) to 20 subjects. Each subject includes two trials, and each trial includes 40
290 sweeps of pain stimulation. In this research work, a dataset of all RGB images from 20 subjects is
291 selected. The number of no pain video sequences are more than others. Therefore, based on the specific
292 character of the database it is likely that any model gets biased towards the prediction of no-pain at the
293 cost of missing pain frames. Using imbalance data is basically intentionally biasing data to get an
294 interesting result. To deal with this issue, in this study the database was balanced using under
295 resampling techniques to reduce the majority class (no-pain class). So, some no pain sequences have
296 been removed.

297 The resampling technique was applied on the selected dataset since a few subjects were missing for
298 some sweeps and there was not an equal proportion for each class as well. Therefore, the under-sample
299 technique was applied to reduce the majority class, and some no painful sequences (Lable0) were
300 removed. The total of 34800 video frames is selected for experimentation in this research. Fig. 6 shows
301 the samples of the selected dataset.

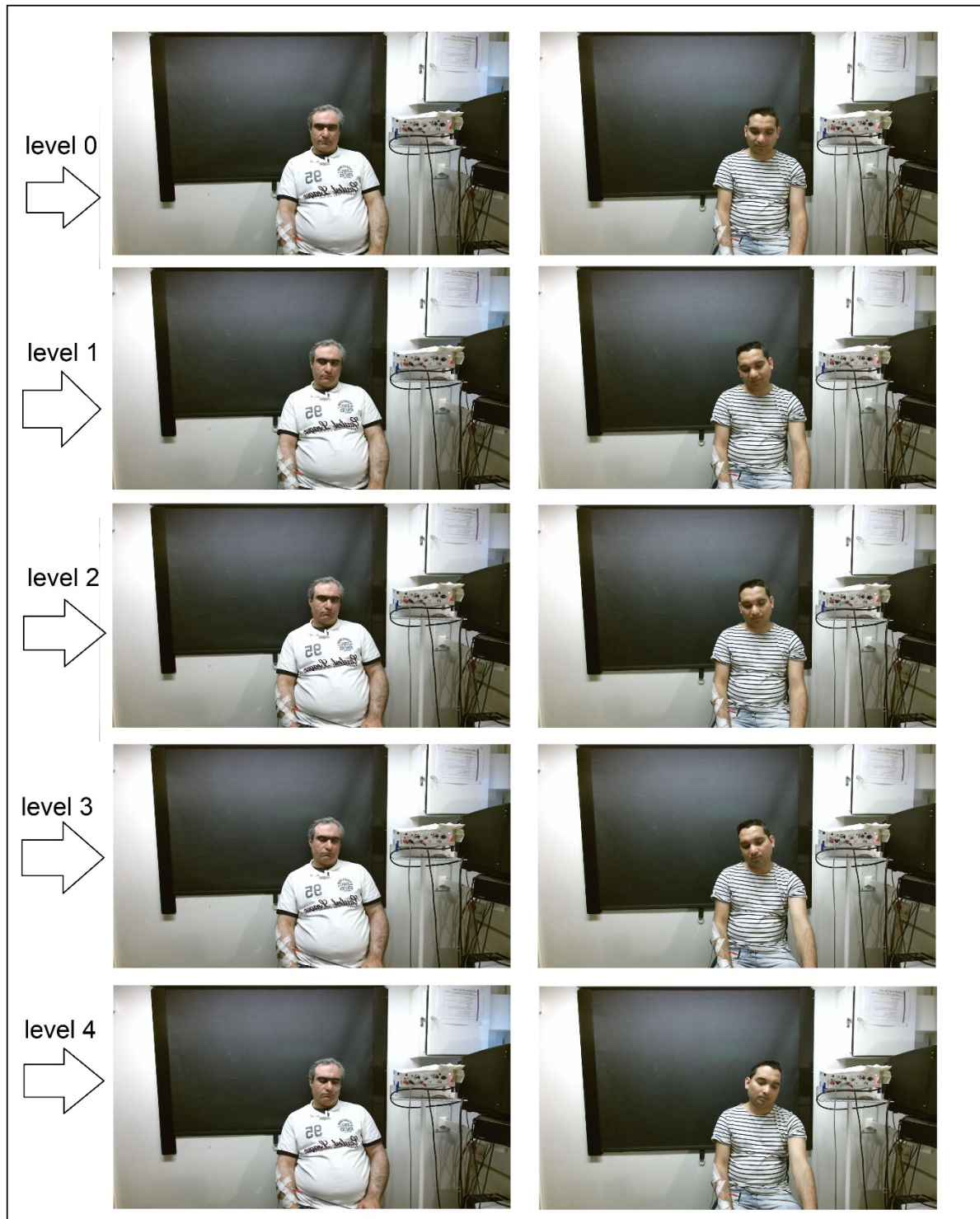


Fig. 6. Samples of selected dataset of MIntPAIN database [2, 16].

302

303

304 The selected dataset was pre-processed by removing noises and backgrounds from each video frames.

305 The pre-processing includes face detecting, cropping, and centralizing applied on the video frames.

306 Then, the images were normalized before feeding images to the proposed model. Moreover, the

307 OpenCV face recognition algorithm was used to detect faces from noisy pictures. Then, face detected

308 images were cropped and centralizing (see Fig. 7). Finally, the pre-processed data was reshaped to

309 224×224×3 dimensions to transfer into VGGFace pre-trainer. To normalize the pixel values for both
 310 train and test datasets, the data was rescaled to the range [0,1]. This includes converting the data type
 311 from integer to floats and splitting the pixel values by the highest value [54].

312
$$\text{Normalize: } R \rightarrow R: x \rightarrow \frac{x}{d} \quad d = \max_{x \in \text{image}} \|x\| \quad (6)$$



313
 314 **Fig. 7.** Examples of video frames per 5 level after removing backgrounds, cropping, and resizing.

315 **4.2 The UNBC-McMaster Shoulder Pain database**

316 To prove the generality of the proposed EDLM model, the experiment was conducted on the UNBC-
 317 McMaster Shoulder Pain dataset [17] and competitive results were obtained. The database provides the
 318 image's frames of video sequences from patients suffering shoulder pain. Each frame of the database
 319 was coded in terms of PSPI score among 0 to 15 scales. The database provides 200 sequences across
 320 25 subjects, which totals 48,398 image frames. **The number of no pain images PSPI score labels are**
 321 **higher than the other labels and the number of images with the PSPI labels greater than 6 are only a few**
 322 **within this database. Therefore, based on the specific character of the database it is likely that any model**
 323 **can be biased towards the prediction of no-pain at the cost of missing pain frames. Using imbalance**

324 data is basically intentionally biasing data to get an interesting result. To deal with this issue, in this
 325 study the database was balanced using under resampling techniques to reduce the majority class (no-
 326 pain class). We balanced the database is by under-resampling technique to reduce the majority class
 327 (no-pain class) and 10,783 images were thus employed in this research. For classifying pain into five
 328 levels, the database was divided into five parts including (PSPI = 0), (PSPI = 1), (PSPI = 2 and 3), (PSPI
 329 = 4 and 5) and (PSPI > = 6). Fig. 8 shows samples of the UNMC-McMaster Shoulder Pain database for
 330 some classes.



331
 332 **Fig. 8** Image frame samples of the UNMC-McMaster Shoulder Pain Achieve database [17].

333 4.2 The evaluation metrics

334 To train, test, and evaluate the proposed EDLM ensemble model, this section provides several empirical
 335 results of the modelling experiments carried out and evaluations in comparison with other models
 336 developed during experimentation and previous researches using MIntPAIN database. To enable
 337 rigorous evaluations of the proposed EDLM model in respect to the counterpart models, several
 338 performance evaluations measures, including the Classification Mean Absolute Error (MAE), Mean
 339 Squared Error (MSE), Accuracy, AUC and F-score were utilized. Mathematically, the metrics are stated
 340 as follows where:

341 $e = e_{experimental} - e_{true}$ and N = number of errors:

$$342 \quad MAE = \frac{1}{N} \sum_{i=1}^N |e_i| \quad (11)$$

$$343 \quad MSE = \frac{1}{N} \sum_{i=1}^N (e_i)^2 \quad (12)$$

344 We used some metrics such as accuracy f-measure to measure performance of the algorithm. The
 345 mathematical formula of them is as following.

$$346 \quad Accuracy = \frac{TP + TN}{TP + TN + FP + FN} \quad (13)$$

$$347 \quad Precision = \frac{TP}{TP + FP} \quad (14)$$

$$348 \quad Recall = \frac{TP}{TP + FN} \quad (15)$$

$$349 \quad F = 2 \times \frac{Recall \times Precision}{Recall + Precision} \quad (16)$$

$$350 \quad TPR = \frac{TP}{(FN + TP)} \quad (17)$$

$$351 \quad FPR = \frac{FP}{(TN + FP)} \quad (18)$$

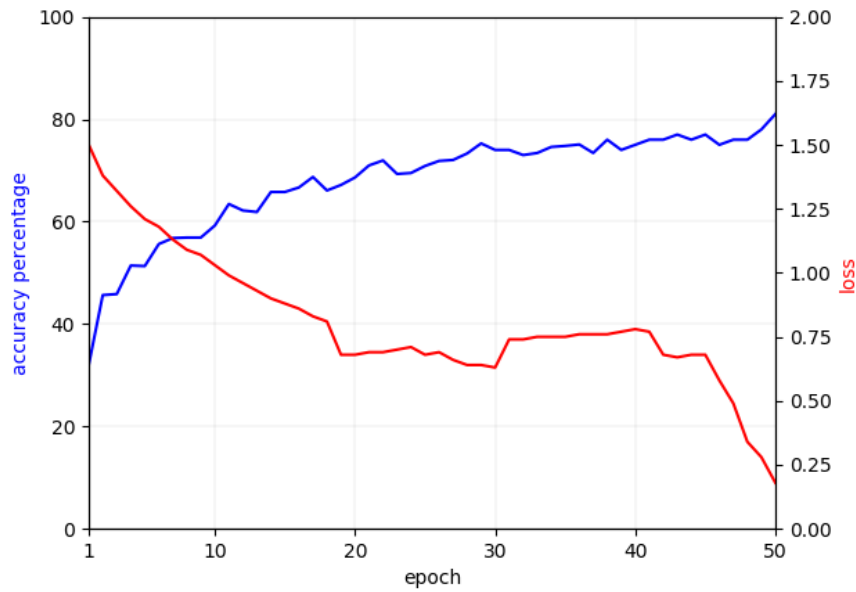
352 Where True Positive (TP) is the cases are predicted YES, and the actual output is YES and True
 353 Negatives (TN) is the cases are predicted NO, and the actual output is NO. False Positives (FP) is the
 354 cases are predicted YES, and the actual output is NO. False Negatives (FN) is the cases are predicted
 355 NO, and the actual output is YES [55]. True Positive Rate (TPR) corresponds to the proportion of
 356 positive data points that are correctly considered as positive, with respect to all positive data points.
 357 False Positive Rate (FPR) corresponds to the proportion of negative data points that are mistakenly
 358 considered as positive, with respect to all negative data points.

359 **5. Results and discussions**

360 In this section we train and test our proposed framework in two different databases includes MIntPain
 361 and UNBC-McMaster Shoulder Pain databases. Next, the evaluated results compared with the baseline
 362 model and the state-of-the-art researches.

363 **5.1 The MIntPAIN database results**

364 The features have been extracted and selected by early fusion finetuned VGGFace and PCA. The early
 365 fusion algorithm to reach its best performance used 50 epochs. Fig. 9 illustrates the accuracy and the
 366 loss error encountered in the early fusion in the EDLM model. This figure shows the average number
 367 of the accuracy for 10 cross validation during 50 epochs. As it is indicated in Fig.9 the accuracy level
 368 has been reached to the its highest level by 81% in epoch = 50. It has been started from 32% in epoch
 369 1 and gradually has been increased. The red line in this figure shows the loss value average for 10 Cross
 370 validation and shows a decreasing amount in loss level by increasing epoch. The loss has been reached
 371 in the lowest level by 0.18 in epoch 50.



372

373
374

Fig. 9. Accuracy and loss error during 50 epochs in the early fusion of the EDLM model in the MIntPAIN database.

375

376

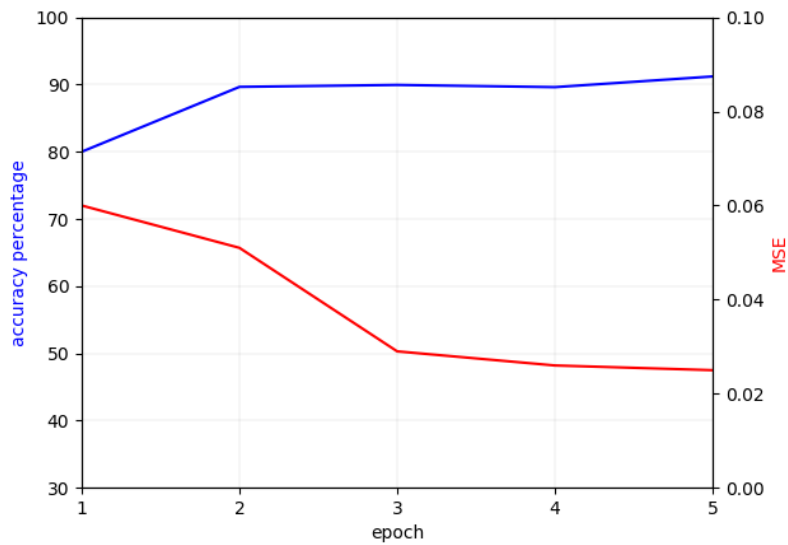
377

378

379

380

Later, the proposed classifier which is late fusion here has been trained and tested by selected features. Fig. 10 shows the accuracy and loss level during 5 epochs in average of 10 cross validation for late fusion. At first, accuracy has been started by 81% and then from the second epoch it reaches to 92.26% in epoch 5. The red graph in Fig. 10 shows the MSE level in average. As it is shown in this graph in epoch one the MSE equal to 0.06 but by repeating testing and training in epoch 5 it reached to its lowest level by 0.028.



381

382

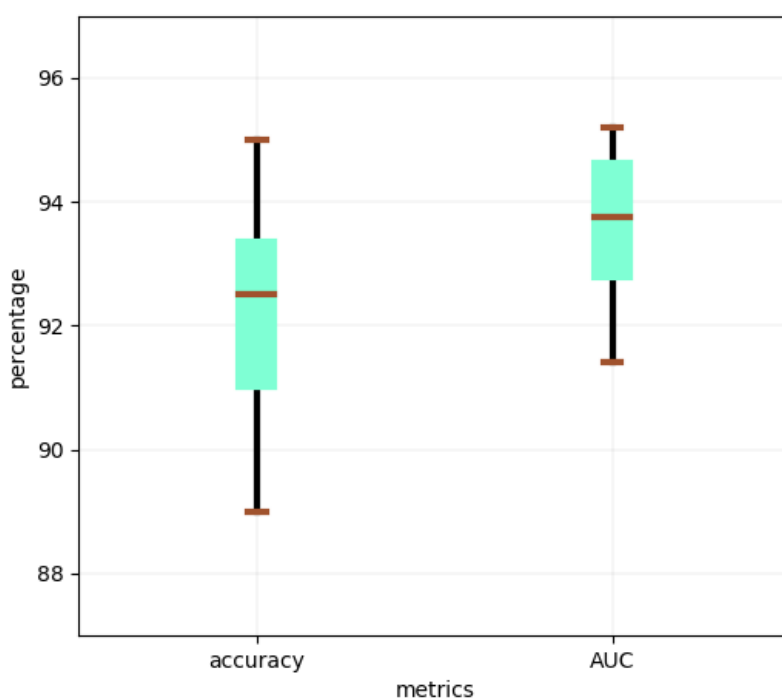
Fig. 10. Accuracy and MSE during 5 epochs in the late fusion of the EDLM model in the MIntPAIN database.

383 Table 2 and Fig. 11 indicate the obtained results of the proposed EDLM on the MIntPAIN database
 384 measured by accuracy, AUC, MAE, and MSE based on 10-fold cross validation.

385 **Table 2.** The average performance, best result, and worst results of the proposed model (EDLM) on MIntPAIN
 386 database for 10-fold cross validation.

| Results | MSE | MAE | Accuracy | AUC |
|---------|---------|--------|----------|--------|
| Average | 0.0245 | 0.0341 | 92.26% | 93.67% |
| Best | 0.02102 | 0.028 | 95% | 95.2% |
| Worst | 0.03056 | 0.039 | 89% | 91.4% |

387



388

389 **Fig. 11.** Box plots of Accuracy and AUC for the proposed EDLM model in the MIntPAIN database.

390 Fig. 11 displays the accuracy and AUC of the proposed EDLM model in the box plot. It shows the
 391 distribution of data based on minimum, first quartile, median, third quartile, and maximum. Median is
 392 shown as yellow, minimum and maximum shown as blue lines. Median is demonstrated by the middle
 393 value of the accuracy and AUC. The first quartile shows the middle number between the smallest
 394 number and the median of the dataset. Third quartile shows the middle value between the median and
 395 the highest value of the dataset.

396 Other popular evaluation metrics such as f-score and precision also have been exploited to evaluate the
 397 performance of the proposed EMDL model and the results show optimum and effective ranges of
 398 effectiveness per each class. The performance of the proposed EDLM model shows a significant
 399 correctness per five classes measured by AUC ROC (Receiver Operating Characteristics) curve metric.

400 Table 3 indicates the accuracy, AUC, f-score, and precision for each class with no-pain, pain level 1,
 401 pain level 2, pain level 3, and pain level 4.

402 **Table 3.** Average pain level per five classes based on accuracy, f-score, precision, AUC metrics in the
 403 MIntPAIN database.

| Metrics | No pain | Pain 1 | Pain 2 | Pain 3 | Pain 4 |
|----------------|----------------|---------------|---------------|---------------|---------------|
| AUC | 87.3% | 84% | 85% | 89% | 91% |
| Precision | 85.2% | 85% | 83% | 88% | 88% |
| f-score | 86% | 82% | 82.2% | 86.2% | 90% |
| Accuracy | 92.4% | 89% | 88% | 93% | 92% |

404 The accuracy of the proposed EDLM model is assessed by TPR and FPR analysis and results show
 405 effectiveness of it by obtaining higher values for TPR and lower values for FPR in five classes.

406 5.2 The UNBC-McMaster Shoulder Pain database results

407 To prove the generality of the proposed EDLM model, the experiment was conducted on the UNBC-
 408 McMaster Shoulder Pain dataset and the obtained results indicate that the proposed EDLM framework
 409 has high performance in this database. In this database we used PSPI labels per each frame. To enable
 410 rigorous evaluations of the proposed EDLM model in respect to the counterpart models, several
 411 performance evaluations measures, including the MAE, MSE, Accuracy, and AUC were utilized. Table
 412 4 indicates the obtained results of the proposed EDLM on the UNBC-McMaster Shoulder Pain database
 413 measured by accuracy, AUC, MAE, and MSE based on 10-fold cross validation.

414 **Table 4.** The average performance of the proposed model (EDLM) in the UNBC-McMaster Shoulder Pain
 415 database for 10-fold cross validation.

| MSE | MAE | Accuracy | AUC |
|------------|------------|-----------------|------------|
| 0.081 | 0.103 | 86% | 90.5% |

416 5.3 Discussion

417 We compared the obtained results from the EDLM with a baseline model which is designed based on a
 418 standard VGG-Face and one stream LSTM model. Table 5 shows the comparison results obtained by
 419 the EDLM proposed framework with the baseline model results. As it is indicated in this table the
 420 proposed EDLM has higher performance than the standard baseline model.

421 **Table 5.** The comparison of the obtained AUC and accuracy from the EDLM and the baseline model in the
 422 MIntPAIN database.

| Classification models | AUC | Accuracy |
|--------------------------------|---------------|-----------------|
| VGGFace + 1 stream LSTM | 87% | 83.4% |
| <i>The proposed EDLM model</i> | <i>93.67%</i> | <i>92.26%</i> |

423 The time complexity of the proposed EDLM algorithm has also been measured in two databases and
 424 compared with two other baseline models which have been developed during experimental. Table 6
 425 shows the learning time of the EDLM for two databases in comparison with two different baseline
 426 models. As is indicated in Table 6, the total time complexity of the proposed EDLM algorithm for the
 427 UNBC-McMaster Shoulder Pain database is 5900 s and the time complexity of it for the MIntPAIN
 428 database is 41700 s.

429 As a result, the most time-consuming section of the EDLM is feature extraction section and adding
 430 more streams in the classifier has not affected the algorithm speeds and efficiency. On the other hand,
 431 the selected database and the required number of epochs are important factors which affect the
 432 complexity and learning time of the algorithm.

433 Table 6. The time complexity of the proposed EDLM in compare with other baseline algorithm in the UNBC-
 434 McMaster Shoulder Pain database and MIntPAIN database.

| Models | Database | Early fusion Time complexity (based on second) and number of applied epochs | Late fusion Time complexity (based on second) and number of applied epochs | Sum of the Time complexity |
|---|---------------------------|--|---|---|
| VGGFace + 1 stream LSTM | UNBC- McMaster | 10400 / 5 | 560 / 5 | 10960 |
| VGGFace + 1 stream LSTM | MIntPAIN | 108000 / 50 | 1600 / 5 | 109600 |
| VGGFace + PCA + 1 stream LSTM | UNBC- McMaster | 5300 / 5 | 560 / 5 | 5860 |
| VGGFace + PCA + 1 stream LSTM | MIntPAIN | 40000 / 50 | 1600 / 5 | 41600 |
| <i>Proposed EDLM (VGGFace + PCA + 3 stream CNN- BiLSTM)</i> | <i>UNBC- McMaster</i> | <i>5300 / 5</i> | <i>600 / 5</i> | <i>5900</i> |
| <i>Proposed EDLM (VGGFace + PCA + 3 stream CNN- BiLSTM)</i> | <i>MIntPAIN</i> | <i>40000 / 50</i> | <i>1700 / 5</i> | <i>41700</i> |

435 The EDLM model demonstrated the highest performance in comparison with the other models and the
 436 state-of-the-art results. Table 7 indicates a comparison of the proposed EDLM method scores against
 437 other state-of-the-art procedures in pain intensity recognition. In this table the obtained results trained
 438 and tested in the both databases compared with the other research works.

439 **Table 7.** Comparing the proposed EDLM with the other state-of-the-art procedures in pain intensity recognition.

| Ref | Pain Level | AUC (%) | Classifier | Accuracy (%) | MSE | Database | Data size |
|----------------------|------------|--------------|-------------------------|--------------|---------------|----------------------|---------------------|
| [17] | 2 | 83.9 | SVM | - | - | UNBC-McMaster | All |
| [27] | 2 | 84.7 | SVM | - | - | UNBC-McMaster | All |
| [31] | 2 | 93.3 | CNN-LSTM | 83.1 | 0.74 | UNBC-McMaster | Down-up |
| [16] | 3 | - | CNN-RNN | 61.9 | - | UNBC-McMaster | Down-up |
| [22] | 2 | - | - | - | 1.54 | UNBC-McMaster | 16657 images |
| [2] | 5 | - | CNN-LSTM | 32.40 | - | MIntPAIN | All |
| [56] | 4 | 98.4 | PCA-CNN-RNN | 91.2 | 0.04 | UNBC-McMaster | Down-up |
| <i>Proposed EDLM</i> | 5 | <i>93.67</i> | <i>Ensemble CNN-RNN</i> | <i>92.26</i> | <i>0.0245</i> | <i>MIntPAIN</i> | <i>34800 images</i> |
| <i>Proposed EDLM</i> | 5 | <i>90.5</i> | <i>Ensemble CNN-RNN</i> | <i>86</i> | <i>0.081</i> | <i>UNBC-McMaster</i> | <i>10783 images</i> |

440 By analysing the results and comparing them with the state-of-the-art results, we can conclude as
 441 follows:

442 1. The proposed new feature extraction model composing fine-tuned VGGFace pre-trained and PCA
 443 significantly increased the performance of the algorithm feature extraction in compare with the standard
 444 VGG-Face.

445 2. The proposed ensemble deep learning model (EDLM) which integrated three independent CNN-
 446 RNN deep learners with vary in weights and structures has high performance in comparison with the
 447 baseline VGG-Face and one stream LSTM model.

448 3. An evaluation of the proposed model through statistical metrics and investigative plots expose that
 449 the ensemble EDLM model generates improved classification compared to the other benchmarked
 450 models in multi classes.

451 4. The proposed EDLM model is the optimum deep learning method resulting in a low qualified error
 452 compared with the other target models in this task.

453 *Although the obtained results from evaluation of the newly developed EDLM model confirm its*
 454 *effectiveness, the feature work can use different frameworks for pain recognition such as the technique*
 455 *introduced in [8] which firstly recognizes the general facial expression, then if it detects pain, then use*
 456 *the authors' proposal to provide fine-grained pain level classification. Deep metric learning methods*
 457 *may also be used to achieve better performance such as Siamese networks [9]. Future work, may also*
 458 *consider loss functions method that perform well on imbalanced datasets [57-61].*

459 There are some limitations in terms of the number of pain datasets from facial expressions in pain
460 detection research. One of the challenges is that most of the research into facial expressions, especially
461 in the area of facial pain detection, currently lacks a standard database. This makes it relatively difficult
462 to train an accurate facial image recognition system that can act as a robust platform for recognizing the
463 pain and modelling the subsequent pain intensity relative to any given facial image.

464 **6. Conclusions and future work**

465 This study was designed to support ongoing efforts in developing artificial intelligence technologies for
466 pain detection using facial expression images, and as such, the work has proposed a newly designed,
467 classification model with an ensemble deep learning approach. The resulting EDLM model therefore
468 integrates the three-stream independent CNN-RNN based networks that are seen to vary in their
469 structure and weights denoting features extracted from facial images. The proposed EDLM model then
470 applied the fine-tuned VGGFace algorithm, integrated with the PCA approach to extract features from
471 facial images. Finally, the ensemble deep learning model that includes three independent CNN-RNN
472 was designed and tested for its classification accuracy.

473 The proposed EDLM model has been evaluated comprehensively through the MIntPAIN and UNBC-
474 McMaster Shoulder Pain datasets. The evaluated results indicate that the proposed ensemble deep
475 learning model has an improved performance relative to the conventional method such as a single hybrid
476 deep learning model adopted for this task. The extensive evaluation of the EDLM model, through
477 statistical metrics and diagnostic plots, reveals its capability to generate superior classification of facial
478 images and its features compared with the other benchmarked models. Therefore, the deep learning
479 EDLM model is found to attain an optimal accuracy evidenced by a relatively lower error compared
480 with the other benchmarked models. The promising capabilities of the deep learning EDLM model
481 indicates that a future study may advance this algorithm in different types of pain face images and video
482 frame databases to further accelerate the efficiency and effectiveness of feature extracting of images for
483 more broader real-time applications in health informatics and medical diagnosis areas.

484 **Acknowledgments**

485 This research has been supported by an Australian Government Research Training Program Scholarship
486 and was funded by the Australian Research Council (ARC) (grant number LP150100673) supported by
487 Nexus eCare Pty Ltd. The authors declare no conflict of interest.

488 **References**

- 489 [1] D. L. Martinez, O. Rudovic, and R. Picard, "Personalized automatic estimation of self-reported
490 pain intensity from facial expressions," presented at the 2017 IEEE Conference on Computer
491 Vision and Pattern Recognition Workshops (CVPRW), Honolulu, Hawaii, 2017.
- 492 [2] M. A. Haque *et al.*, "Deep multimodal pain recognition: a database and comparison of spatio-
493 temporal visual modalities," in *2018 13th IEEE International Conference on Automatic Face &*

- 494 *Gesture Recognition (FG 2018)*, Xian, China, 2018: IEEE, pp. 250-257, doi:
495 10.1109/FG.2018.00044.
- 496 [3] C. M. A. Ilyas, M. A. Haque, M. Rehm, K. Nasrollahi, and T. B. Moeslund, "Facial Expression
497 Recognition for Traumatic Brain Injured Patients," in *VISIGRAPP (4: VISAPP)*, 2018, pp. 522-
498 530.
- 499 [4] J. Klonovs *et al.*, *Distributed computing and monitoring technologies for older patients*.
500 Switzerland AG.: Springer, 2016.
- 501 [5] P. Ekman and W. V. Friesen, *Facial action coding system: Investigator's guide*. Palo Alto, CA.:
502 Consulting Psychologists Press, 1978.
- 503 [6] K. M. Prkachin and P. E. Solomon, "The structure, reliability and validity of pain expression:
504 Evidence from patients with shoulder pain," *Pain*, vol. 139, no. 2, pp. 267-274, 2008.
- 505 [7] M. Kunz, A. Gruber, and S. Lautenbacher, "Sex differences in facial encoding of pain," *The*
506 *Journal of Pain*, vol. 7, no. 12, pp. 915-928, 2006.
- 507 [8] C. Zhang, P. Wang, K. Chen, and J.-K. Kämäräinen, "Identity-aware convolutional neural
508 networks for facial expression recognition," *Journal of Systems engineering and Electronics*,
509 vol. 28, no. 4, pp. 784-792, 2017.
- 510 [9] X. Liu, B. Vijaya Kumar, J. You, and P. Jia, "Adaptive deep metric learning for identity-aware
511 facial expression recognition," in *Proceedings of the IEEE Conference on Computer Vision and*
512 *Pattern Recognition Workshops*, 2017, pp. 20-29.
- 513 [10] A. Krizhevsky, I. Sutskever, and G. E. Hinton, "Imagenet classification with deep convolutional
514 neural networks," in *Advances in neural information processing systems*, Nevada, USA, 2012,
515 pp. 1097-1105.
- 516 [11] W. Li, R. Zhao, T. Xiao, and X. Wang, "Deepreid: Deep filter pairing neural network for person
517 re-identification," in *Proceedings of the IEEE conference on computer vision and pattern*
518 *recognition*, Columbus, Ohio, 2014, pp. 152-159.
- 519 [12] G. Tsoumakas and I. Vlahavas, "Random k-labelsets: An ensemble method for multilabel
520 classification," in *European conference on machine learning*, Warsaw, Poland 2007: Springer,
521 pp. 406-417.
- 522 [13] B. Liu, Q. Cui, T. Jiang, and S. Ma, "A combinational feature selection and ensemble neural
523 network method for classification of gene expression data," *BMC bioinformatics*, vol. 5, no. 1,
524 p. 136, 2004.
- 525 [14] T. G. Dietterich, "Ensemble methods in machine learning," in *International workshop on*
526 *multiple classifier systems*, Günzburg, Germany 2000: Springer, pp. 1-15, doi:
527 https://doi.org/10.1007/3-540-45014-9_1.
- 528 [15] K. Simonyan and A. Zisserman, "VERY DEEP CONVOLUTIONAL NETWORKS FOR LARGE-SCALE
529 IMAGE RECOGNITION," in *ICLR*, San Diego, 2015, pp. 1-14.
- 530 [16] M. Bellantonio *et al.*, "Spatio-temporal pain recognition in cnn-based super-resolved facial
531 images," in *Video Analytics. Face and Facial Expression Recognition and Audience*
532 *Measurement*, Cancun, Mexico, 2016: Springer, pp. 151-162.
- 533 [17] P. Lucey, J. F. Cohn, K. M. Prkachin, P. E. Solomon, and I. Matthews, "Painful data: The UNBC-
534 McMaster shoulder pain expression archive database," in *Face and Gesture 2011*, Santa
535 Barbara, CA, USA 2011: IEEE, pp. 57-64.
- 536 [18] Y. Taigman, M. Yang, M. A. Ranzato, and L. Wolf, "Deepface: Closing the gap to human-level
537 performance in face verification," in *Proceedings of the IEEE conference on computer vision*
538 *and pattern recognition*, Columbus, Ohio, 2014, pp. 1701-1708.
- 539 [19] Y. Sun, X. Wang, and X. Tang, "Deeply learned face representations are sparse, selective, and
540 robust," in *Proceedings of the IEEE conference on computer vision and pattern recognition*,
541 Boston, Massachusetts, 2015, pp. 2892-2900.
- 542 [20] F. Hu, G.-S. Xia, J. Hu, and L. Zhang, "Transferring deep convolutional neural networks for the
543 scene classification of high-resolution remote sensing imagery," *Remote Sensing*, vol. 7, no.
544 11, pp. 14680-14707, 2015, doi: <https://doi.org/10.3390/rs71114680>.

- 545 [21] C. Szegedy et al., "Going deeper with convolutions," in *Proceedings of the IEEE conference on*
546 *computer vision and pattern recognition*, 2015, Boston, Massachusetts, pp. 1-9.
- 547 [22] J. Zhou, X. Hong, F. Su, and G. Zhao, "Recurrent convolutional neural network regression for
548 continuous pain intensity estimation in video," in *Proceedings of the IEEE Conference on*
549 *Computer Vision and Pattern Recognition Workshops*, Honolulu, Hawaii, USA, 2016: IEEE, pp.
550 84-92.
- 551 [23] J. Schmidhuber, "Deep learning in neural networks: An overview," *Neural networks*, vol. 61,
552 pp. 85-117, 2015.
- 553 [24] F. A. Gers and E. Schmidhuber, "LSTM recurrent networks learn simple context-free and
554 context-sensitive languages," *IEEE Transactions on Neural Networks*, vol. 12, no. 6, pp. 1333-
555 1340, 2001, doi: 10.1109/72.963769.
- 556 [25] C. Dyer, M. Ballesteros, W. Ling, A. Matthews, and N. A. Smith, "Transition-based dependency
557 parsing with stack long short-term memory," in *ACL 2015*, Beijing, 2015.
- 558 [26] A. B. Ashraf et al., "The painful face-pain expression recognition using active appearance
559 models," *Image and vision computing*, vol. 27, no. 12, pp. 1788-1796, 2009, doi:
560 <https://doi.org/10.1016/j.imavis.2009.05.007>.
- 561 [27] P. Lucey et al., "Automatically Detecting Pain in Video Through Facial Action Units," *IEEE*
562 *Transactions on Systems, Man, and Cybernetics, Part B: Cybernetics*, vol. 41, 3, pp. 664-674,
563 2011.
- 564 [28] G. Littlewort-Ford, M. S. Bartlett, and J. R. Movellan, "Are your eyes smiling? detecting
565 genuine smiles with support vector machines and gabor wavelets," in *Proceedings of the 8th*
566 *Joint Symposium on Neural Computation*, 2001, UC San Diego.
- 567 [29] C. Shan, "Learning local binary patterns for gender classification on real-world face images,"
568 *Pattern recognition letters*, vol. 33, no. 4, pp. 431-437, 2012.
- 569 [30] G. Hinton, N. Srivastava, and K. Swersky, "Neural networks for machine learning lecture 6a
570 overview of mini-batch gradient descent," 2012.
- 571 [31] P. Rodriguez et al., "Deep pain: Exploiting long short-term memory networks for facial
572 expression classification," *IEEE transactions on cybernetics*, no. 99, pp. 1-11, 2017.
- 573 [32] G. Bargshady, J. Soar, X. Zhou, R. C. Deo, F. Whittaker, and H. Wang, "A joint deep neural
574 network model for pain recognition from face," in *Proceedings of the 4th IEEE International*
575 *Conference on Computer and Communication Systems (ICCS 2019)*, Singapore, 2019: IEEE
576 Press, pp. 52-56.
- 577 [33] J. Egede, M. Valstar, M. T. Torres, and D. Sharkey, "Automatic Neonatal Pain Estimation: An
578 Acute Pain in Neonates Database," in *2019 8th International Conference on Affective*
579 *Computing and Intelligent Interaction (ACII)*, 2019: IEEE, pp. 1-7, doi:
580 10.1109/ACII.2019.8925480.
- 581 [34] Z. Chen, R. Ansari, and D. Wilkie, "Learning Pain from Action Unit Combinations: A Weakly
582 Supervised Approach via Multiple Instance Learning," *IEEE Transactions on Affective*
583 *Computing*, 2019, doi: 10.1109/TAFFC.2019.2949314.
- 584 [35] P. Werner, D. Lopez-Martinez, S. Walter, A. Al-Hamadi, S. Gruss, and R. Picard, "Automatic
585 Recognition Methods Supporting Pain Assessment: A Survey," *IEEE Transactions on Affective*
586 *Computing*, 2019.
- 587 [36] Y. Freund and R. E. Schapire, "A decision-theoretic generalization of on-line learning and an
588 application to boosting," *Journal of computer and system sciences*, vol. 55, no. 1, pp. 119-139,
589 1997, doi: https://doi.org/10.1007/3-540-59119-2_166.
- 590 [37] R. Minetto, M. P. Segundo, and S. Sarkar, "Hydra: an ensemble of convolutional neural
591 networks for geospatial land classification," *IEEE Transactions on Geoscience and Remote*
592 *Sensing*, vol. 57, no. 9, pp. 6530 - 6541, 2019.
- 593 [38] C. Ding and D. Tao, "Trunk-branch ensemble convolutional neural networks for video-based
594 face recognition," *IEEE transactions on pattern analysis and machine intelligence*, vol. 40, no.
595 4, pp. 1002-1014, 2017, doi: 10.1109/TPAMI.2017.2700390.

- 596 [39] O. M. Parkhi, A. Vedaldi, and A. Zisserman, "Deep face recognition," in *bmvc*, Swansea, UK,
597 2015, vol. 1, no. 3, p. 6.
- 598 [40] A. J. C. SHARKEY, "On combining artificial neural nets," *Connection Science*, vol. 8, no. 3-4, pp.
599 299-314, 1996.
- 600 [41] L. K. Hansen and P. Salamon, "Neural network ensembles," *IEEE Transactions on Pattern
601 Analysis & Machine Intelligence*, no. 10, pp. 993-1001, 1990, doi: 10.1109/34.58871.
- 602 [42] J. Xie, B. Xu, and Z. Chuang, "Horizontal and vertical ensemble with deep representation for
603 classification," in *ICML 2013*, Atlanta, 2013.
- 604 [43] A. Gulli and S. Pal, *Deep Learning with Keras*. Birmingham, UK: Packt Publishing Ltd, 2017.
- 605 [44] J. Ma and Y. Yuan, "Dimension reduction of image deep feature using PCA," *Journal of Visual
606 Communication and Image Representation*, vol. 63, p. 102578, 2019.
- 607 [45] J. Li, B. Zhao, H. Zhang, and J. Jiao, "Face recognition system using svm classifier and feature
608 extraction by pca and lda combination," in *2009 International Conference on Computational
609 Intelligence and Software Engineering*, Wuhan, China, 2009: IEEE, pp. 1-4, doi:
610 10.1109/CISE.2009.5364125.
- 611 [46] R. C. Damale and B. V. Pathak, "Face Recognition Based Attendance System Using Machine
612 Learning Algorithms," in *2018 Second International Conference on Intelligent Computing and
613 Control Systems (ICICCS)*, Madurai, India 14-15 June 2018 2018: IEEE, pp. 414-419, doi:
614 10.1109/ICCONS.2018.8662938.
- 615 [47] Y. Sun, Y. Chen, X. Wang, and X. Tang, "Deep learning face representation by joint
616 identification-verification," in *the 27th International Conference on Neural Information
617 Processing Systems* Montreal, Canada, 2014, vol. 2: ACM, pp. 1988-1996.
- 618 [48] I. Goodfellow, Y. Bengio, and A. Courville, *Deep learning*. MIT press, 2016.
- 619 [49] M. F. Sanner, "Python: a programming language for software integration and development,"
620 *J Mol Graph Model*, vol. 17, no. 1, pp. 57-61, 1999.
- 621 [50] N. Ketkar, "Introduction to keras," in *Deep Learning with Python*. Berkeley, CA: Springer, 2017,
622 pp. 97-111.
- 623 [51] M. Abadi et al., "Tensorflow: A system for large-scale machine learning," in *12th Symposium
624 on Operating Systems Design and Implementation* Savannah, GA, 2016, pp. 265-283.
- 625 [52] F. Pedregosa et al., "Scikit-learn: Machine learning in Python," *Journal of machine learning
626 research*, vol. 12, no. Oct, pp. 2825-2830, 2011.
- 627 [53] J. D. Hunter, "Matplotlib: A 2D graphics environment," *Computing in science & engineering*,
628 vol. 9, no. 3, p. 90, 2007, doi: 10.1109/MCSE.2007.55.
- 629 [54] N. Schertler, "Improving JPEG Compression with Regression Tree Fields," Master, Technische
630 Universität Dresden, Dresden Germany, 2014. [Online]. Available: [https://tu-
631 dresden.de/ing/informatik/smt/cgv/ressourcen/dateien/lehre/ergebnisse_studentischer_ar-
632 beiten/masterarbeiten/nico_schertler_ss14/files/Thesis.pdf?lang=en](https://tu-dresden.de/ing/informatik/smt/cgv/ressourcen/dateien/lehre/ergebnisse_studentischer_arbeiten/masterarbeiten/nico_schertler_ss14/files/Thesis.pdf?lang=en)
- 633 [55] D. M. Powers, "Evaluation: from precision, recall and F-measure to ROC, informedness,
634 markedness and correlation," *Journal of Machine Learning Technologies*, vol. 2, no. 1, pp. 37-
635 63, 2011.
- 636 [56] G. Bargshady, X. Zhou, R. C. Deo, J. Soar, F. Whittaker, and H. Wang, "Enhanced deep learning
637 algorithm development to detect pain intensity from facial expression images," *Expert
638 Systems with Applications*, vol. 149, no. 113305, 2020, doi:
639 <https://doi.org/10.1016/j.eswa.2020.113305>.
- 640 [57] T.-Y. Lin, P. Goyal, R. Girshick, K. He, and P. Dollár, "Focal loss for dense object detection," in
641 *Proceedings of the IEEE international conference on computer vision*, 2017, pp. 2980-2988.
- 642 [58] C. Zhang et al., "Multi-imbalance: An open-source software for multi-class imbalance
643 learning," *Knowledge-Based Systems*, vol. 174, pp. 137-143, 2019.
- 644 [59] J. Bi and C. Zhang, "An empirical comparison on state-of-the-art multi-class imbalance learning
645 algorithms and a new diversified ensemble learning scheme," *Knowledge-Based Systems*, vol.
646 158, pp. 81-93, 2018, doi: Show more

647 <https://doi.org/10.1016/j.knosys.2018.05.037>.

648 [60] C. Zhang, J. Bi, and P. Soda, "Feature selection and resampling in class imbalance learning:
649 Which comes first? An empirical study in the biological domain," in *2017 IEEE International
650 Conference on Bioinformatics and Biomedicine (BIBM)*, 2017: IEEE, pp. 933-938.

651 [61] C. Zhang, C. Liu, X. Zhang, and G. Alimpanidis, "An up-to-date comparison of state-of-the-art
652 classification algorithms," *Expert Systems with Applications*, vol. 82, pp. 128-150, 2017.

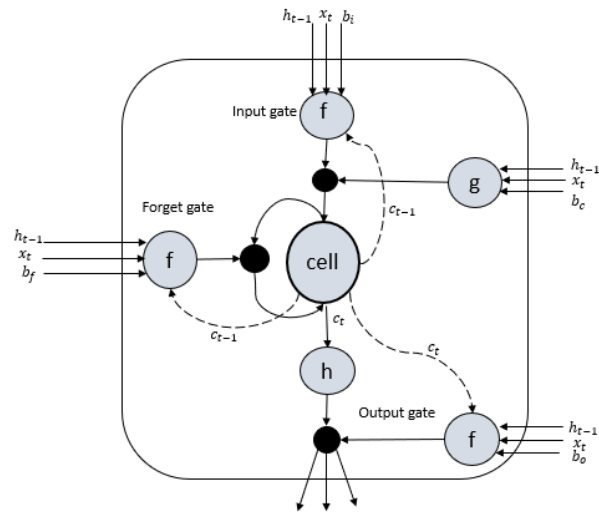


Fig. 1. The architecture of an LSTM unit [23, 24]

Inputs: x_t : Input vector, c_{t-1} : memory from previous block, h_{t-1} : output of previous block, b : Bias Outputs: h_t : the output of current block, c_t : memory from the current block

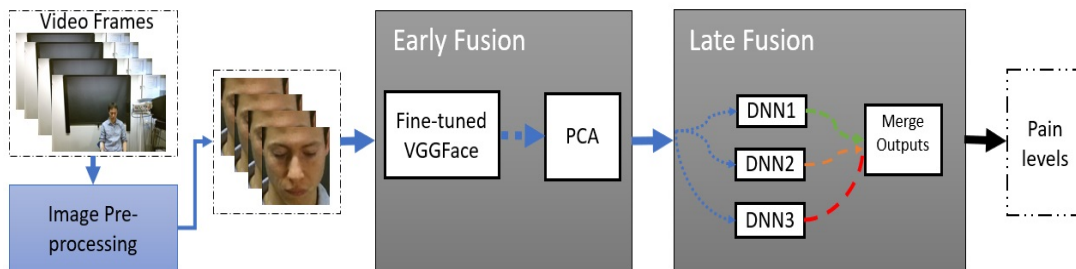


Fig. 2. Block diagram of the proposed ensemble deep learning model (EDLM) to detect pain in multi-classes from facial expressions.

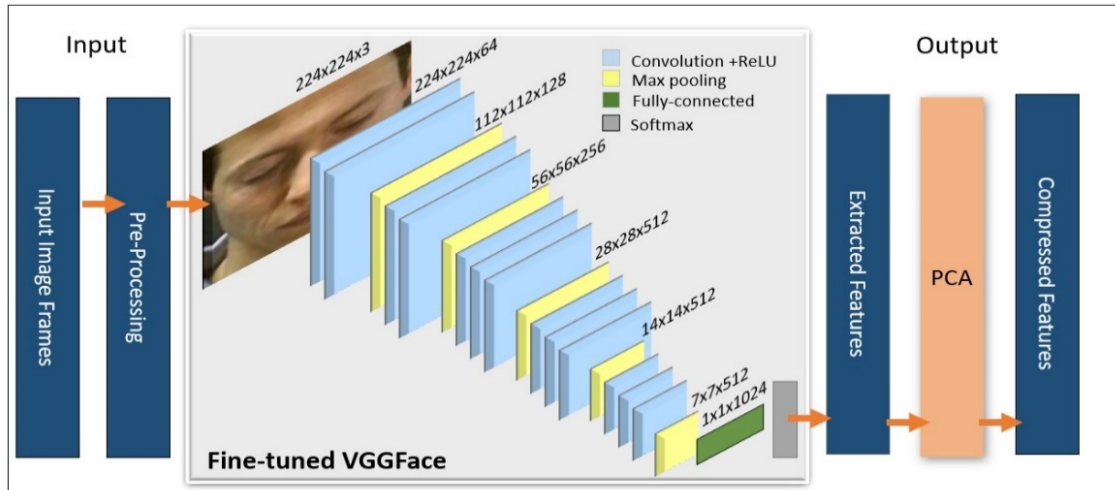


Fig. 3. Early fusion step of the EDLM for feature extraction and selection by integration fine-tuned VGGFace and PCA

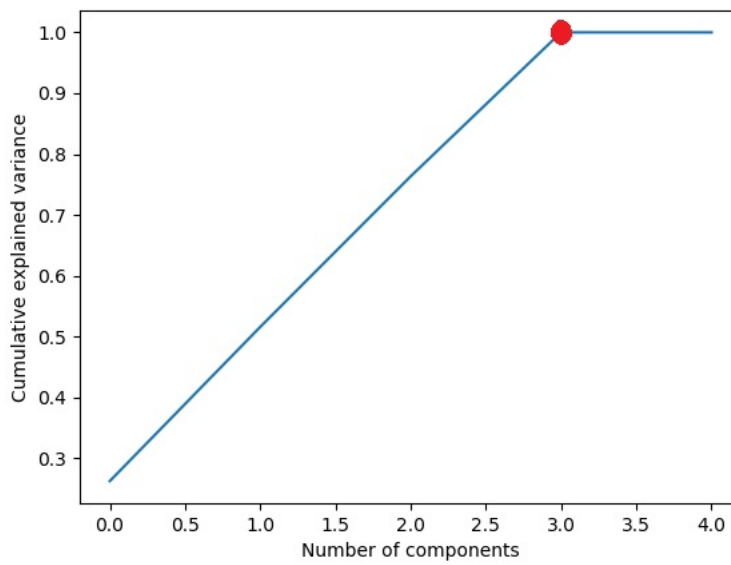


Fig. 4. Number of components to select from extracted features by PCA

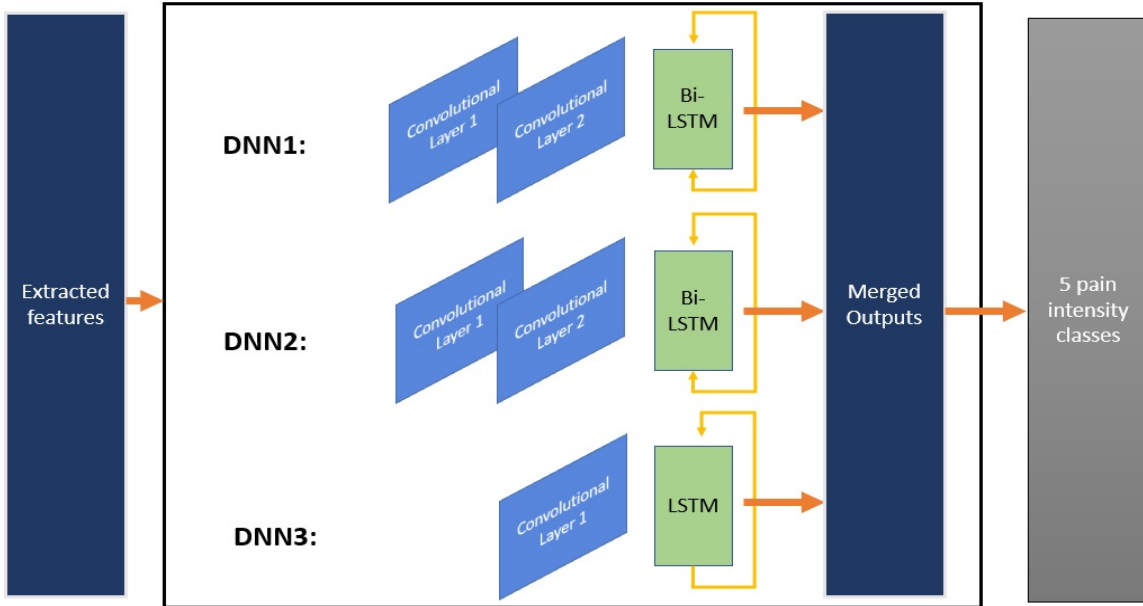


Fig. 5. Late fusion step of the EDLM based on ensemble deep neural network.

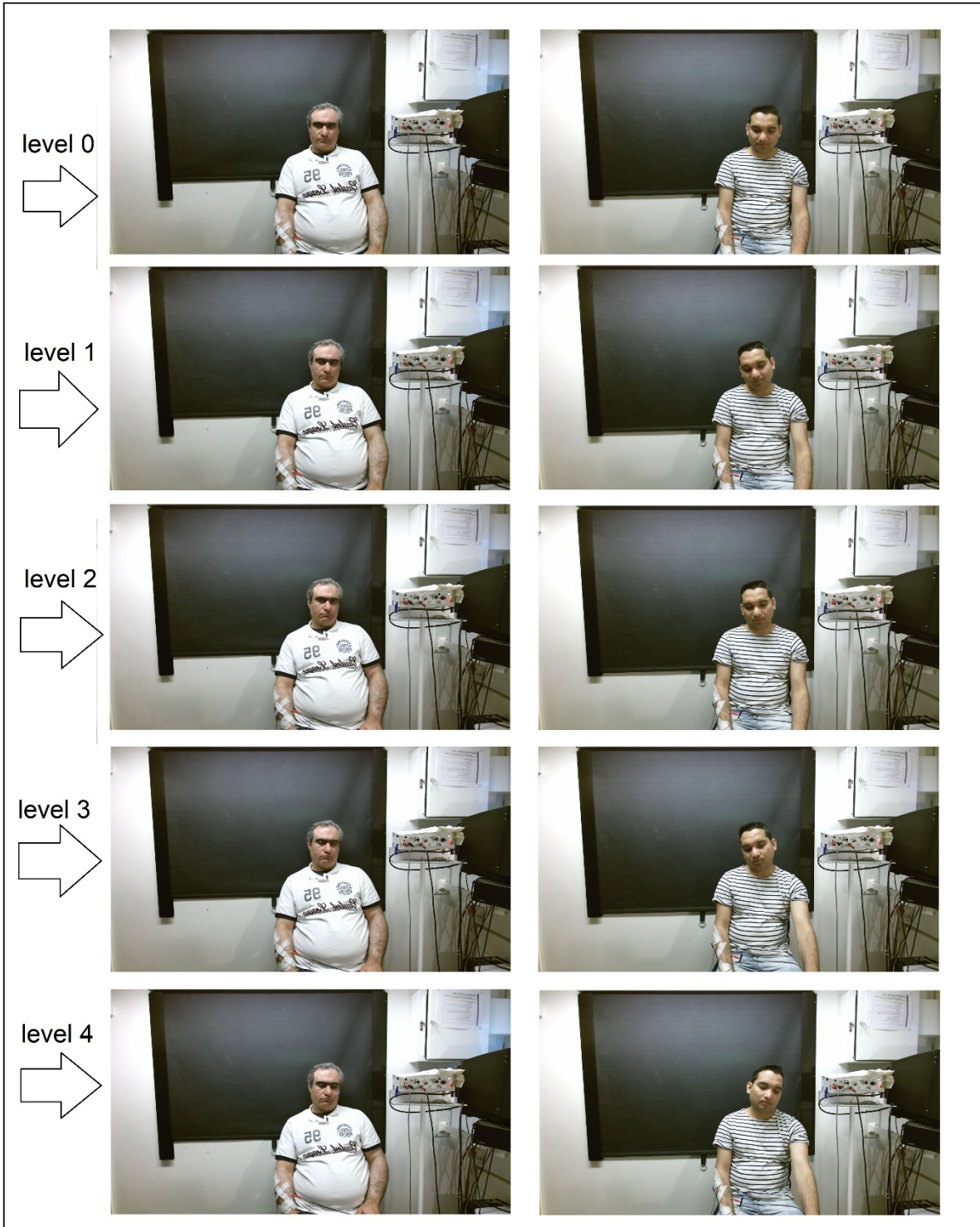


Fig. 6. Samples of selected dataset of MIntPAIN database [2, 16].



Fig. 7. Examples of video frames per 5 level after removing backgrounds, cropping, and resizing.



Fig. 8 Image frame samples of the UNBC-McMaster Shoulder Pain Achieve database [17].

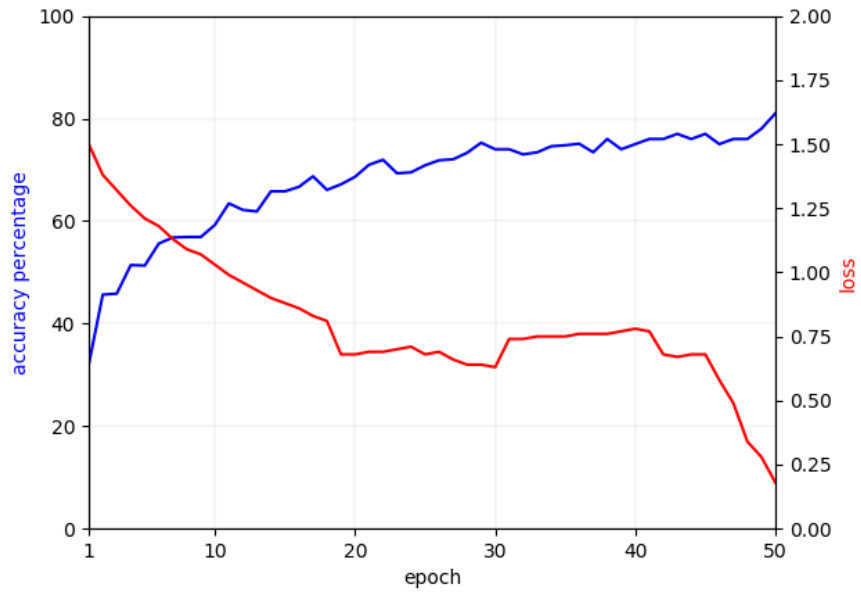


Fig. 9. Accuracy and loss error during 50 epochs in the early fusion of the EDLM model in the MIntPAIN database.

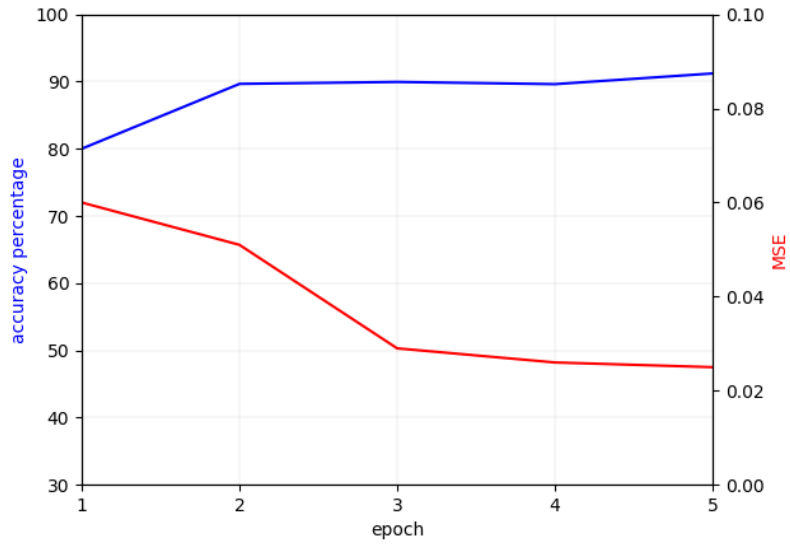


Fig. 10. Accuracy and MSE during 5 epochs in the late fusion of the EDLM model in the MIntPAIN database.

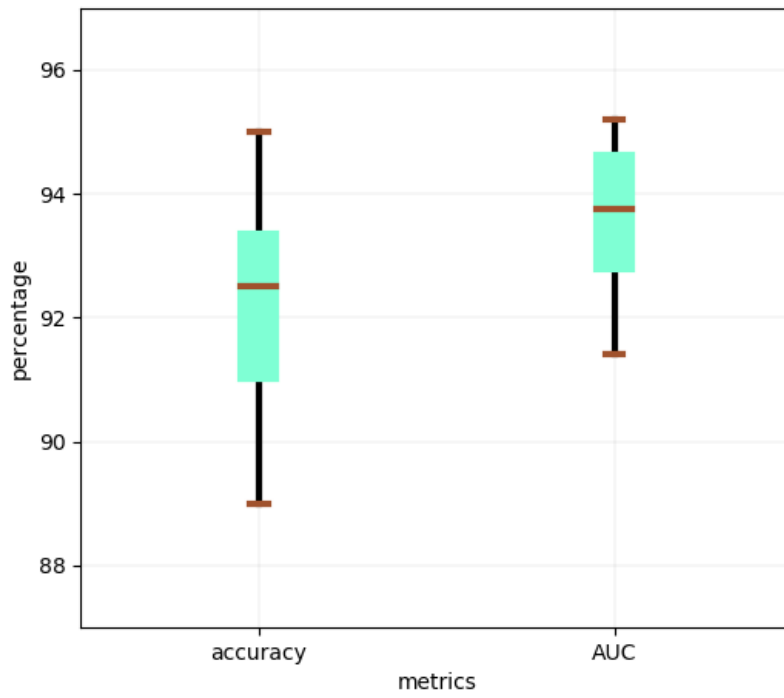


Fig. 11. Box plots of Accuracy and AUC for the proposed EDLM model in the MIntPAIN database.

Table 1. Properties of DNN1, DNN2, and DNN3 proposed in the late fusion stage.

| DNN | Convolution layer 1 | Convolution layer 2 | RNN |
|------|---|--|---|
| DNN1 | type = conv2d, filter number = 256, activation = ReLU, input shape = (1,5) | type = conv2d filter number = 256, activation = ReLU, input shape = (1,5) | type = BiLSTM, filter number = 256, dense = 4096, drop out = 0.5, activation = ReLU |
| DNN2 | type = conv2d, filter number = 128, activation = ReLU, input shape = (1,5) | type = conv2d filter number = 128, activation = ReLU, input shape = (1,5) | type = BiLSTM, filter number = 32, dense = 4096, drop out = 0.5, activation = ReLU |
| DNN3 | type = conv1d, filter number = 256, activation = ReLU, input shape = (1,5) | None | type = BiLSTM, filter number = 128, dense = 4096, drop out = 0.5, activation = ReLU |

Table 2. The average performance, best result, and worst results of the proposed model (EDLM) on MIntPAIN database for 10-fold cross validation.

| Results | MSE | MAE | Accuracy | AUC |
|---------|---------|--------|----------|--------|
| Average | 0.0245 | 0.0341 | 92.26% | 93.67% |
| Best | 0.02102 | 0.028 | 95% | 95.2% |
| Worst | 0.03056 | 0.039 | 89% | 91.4% |

Table 3. Average pain level per five classes based on accuracy, f-score, precision, AUC metrics in the MIntPAIN database.

| Metrics | No pain | Pain 1 | Pain 2 | Pain 3 | Pain 4 |
|-----------|---------|--------|--------|--------|--------|
| AUC | 87.3% | 84% | 85% | 89% | 91% |
| Precision | 85.2% | 85% | 83% | 88% | 88% |
| f-score | 86% | 82% | 82.2% | 86.2% | 90% |
| Accuracy | 92.4% | 89% | 88% | 93% | 92% |

Table 4. The average performance of the proposed model (EDLM) in the UNBC-McMaster Shoulder Pain database for 10-fold cross validation.

| MSE | MAE | Accuracy | AUC |
|------------|------------|-----------------|------------|
| 0.081 | 0.103 | 86% | 90.5% |

Table 5. The comparison of the obtained AUC and accuracy from the EDLM and the baseline model in the MIntPAIN database.

| Classification models | AUC | Accuracy |
|--------------------------------|---------------|-----------------|
| VGGFace + 1 stream LSTM | 87% | 83.4% |
| <i>The proposed EDLM model</i> | <i>93.67%</i> | <i>92.26%</i> |

Table 6. The time complexity of the proposed EDLM in compare with other baseline algorithm in the UNBC-McMaster Shoulder Pain database and MIntPAIN database.

| Models | Database | Early fusion Time complexity (based on second) and number of applied epochs | Late fusion Time complexity (based on second) and number of applied epochs | Sum of the Time complexity |
|---|---------------------------|--|---|---|
| VGGFace + 1 stream LSTM | UNBC- McMaster | 10400 / 5 | 560 / 5 | 10960 |
| VGGFace + 1 stream LSTM | MIntPAIN | 108000 / 50 | 1600 / 5 | 109600 |
| VGGFace + PCA + 1 stream LSTM | UNBC- McMaster | 5300 / 5 | 560 / 5 | 5860 |
| VGGFace + PCA + 1 stream LSTM | MIntPAIN | 40000 / 50 | 1600 / 5 | 41600 |
| <i>Proposed EDLM (VGGFace + PCA + 3 stream CNN- BiLSTM)</i> | <i>UNBC- McMaster</i> | <i>5300 / 5</i> | <i>600 / 5</i> | <i>5900</i> |
| <i>Proposed EDLM (VGGFace + PCA + 3 stream CNN- BiLSTM)</i> | <i>MIntPAIN</i> | <i>40000 / 50</i> | <i>1700 / 5</i> | <i>41700</i> |

Table 7. Comparing the proposed EDLM with the other state-of-the-art procedures in pain intensity recognition.

| Ref | Pain Level | AUC (%) | Classifier | Accuracy (%) | MSE | Database | Data size |
|----------------------|------------|--------------|-------------------------|--------------|---------------|----------------------|---------------------|
| [17] | 2 | 83.9 | SVM | - | - | UNBC-McMaster | All |
| [27] | 2 | 84.7 | SVM | - | - | UNBC-McMaster | All |
| [31] | 2 | 93.3 | CNN-LSTM | 83.1 | 0.74 | UNBC-McMaster | Down-up |
| [16] | 3 | - | CNN-RNN | 61.9 | - | UNBC-McMaster | Down-up |
| [22] | 2 | - | - | - | 1.54 | UNBC-McMaster | 16657 images |
| [2] | 5 | - | CNN-LSTM | 32.40 | - | MIntPAIN | All |
| [56] | 4 | 98.4 | PCA-CNN-RNN | 91.2 | 0.04 | UNBC-McMaster | Down-up |
| <i>Proposed EDLM</i> | 5 | <i>93.67</i> | <i>Ensemble CNN-RNN</i> | <i>92.26</i> | <i>0.0245</i> | <i>MIntPAIN</i> | <i>34800 images</i> |
| <i>Proposed EDLM</i> | 5 | <i>90.5</i> | <i>Ensemble CNN-RNN</i> | <i>86</i> | <i>0.081</i> | <i>UNBC-McMaster</i> | <i>10783 images</i> |

Algorithm 1: The proposed EDLM algorithm

```

1: Procedure EDLM (input, n, j, batch)
2:   Pre-process (input)
3:   for k  $\leftarrow$  0, n do
4:     finetune (VGG-Face)
5:     for epoch  $\leftarrow$  0, j do
6:       features  $\leftarrow$  train (finetune (VGG-Face))
7:     end for
8:     SF  $\leftarrow$  PCA (features)
9:     GN  $\leftarrow$  Calculate (GN)
10:    for epoch  $\leftarrow$  0, j do
11:      o1  $\leftarrow$  DNN1(SF)
12:      o2  $\leftarrow$  DNN2(SF)
13:      o3  $\leftarrow$  DNN3(SF)
14:      out  $\leftarrow$  merge (o1, o2, o3)
15:      out  $\leftarrow$  GN (48)
16:      train (model (SF, out))
17:    end for
18:  end for
19: end procedure

```

Declaration of interests

The authors declare that they have no known competing financial interests or personal relationships that could have appeared to influence the work reported in this paper.

The authors declare the following financial interests/personal relationships which may be considered as potential competing interests: